https://doi.org/10.5194/acp-2020-179
Preprint. Discussion started: 3 April 2020

Atmospheric Chemistry and Physics Discussions
Open Access
EGU

Global dust cycle and uncertainty in CMIP5 models

Chenglai Wu[1,*], Zhaohui Lin[1], and Xiaohong Liu[2]

[1]International Center for Climate and Environment Sciences, Institute of Atmospheric Physics, Chinese Academy of Sciences, Beijing, China

[2]Department of Atmospheric Sciences, Texas A&M University, College Station, USA

* Corresponding author: Chenglai Wu, wuchenglai@mail.iap.ac.cn

Abstract

Dust cycle is an important component of the Earth system and have been implemented into climate models and Earth System Models (ESMs). An assessment of the dust cycle in these models is vital to address the strengths and weaknesses of these models in simulating dust aerosol and its interactions with the Earth system and enhance the future model developments. This study presents a comprehensive evaluation of global dust cycle in 15 models participating in the fifth phase of the Coupled Model Intercomparison Project (CMIP5). The various models are compared with each other and with an aerosol reanalysis as well as station observations of dust deposition and concentrations. The results show that the global dust emission in these models ranges from 735 to 8186 Tg yr^{-1} and the annual mean dust burden ranges from 2.5 to 41.9 Tg, both of which scatter by a factor of about 10-20. The models generally agree with each other and observations in reproducing the "dust belt" that extends from North Africa, Middle East, Central and South Asia, to East Asia, although they differ largely in the

https://doi.org/10.5194/acp-2020-179
Preprint. Discussion started: 3 April 2020

spatial extent of this dust belt. The models also differ in other dust source regions such as North America and Australia, where the contributions of these sources to global dust emissions vary by a factor of more than 500. We suggest that the coupling of dust emission with dynamic vegetation can enlarge the range of simulated dust emission.

For the removal process, all the models estimate that wet deposition is a smaller sink than dry deposition and wet deposition accounts for 12-39 % of total deposition. The models also estimate that most (77-91 %) of dust particles are deposited onto continents and 9-23 % of them are deposited into oceans. A linear relationship between dust burden, lifetime, and fraction of wet deposition to total deposition from these models suggests a general consistency among the models. Compared to the observations, most models reproduce the dust deposition and dust concentrations within a factor of 10 at most stations, but larger biases by more than a factor of 10 are also noted at specific regions and for certain models. These results cast a doubt on the interpretation of the simulations of dust-affected fields in climate models and highlight the need for further improvements of dust cycle especially on dust emission in climate models.

https://doi.org/10.5194/acp-2020-179
Preprint. Discussion started: 3 April 2020

Atmospheric Chemistry and Physics Discussions

1. Introduction

Dust cycle is an important component of the Earth system as it has strong impacts on the Earth environment and climate system (Shao et al., 2011). Dust aerosol in the atmosphere significantly impacts the climate systems via various pathways, such as scattering and absorbing the solar and terrestrial radiation, modifying cloud radiative forcing by acting as cloud condensation nuclei and ice nucleating particles, and reducing the snow albedo when depositing onto snow (Boucher et al., 2013; Forster et al., 2007; Liu, et al., 2012a; Mahowald et al., 2011; Wu et al., 2018a; Rahimi et al., 2019). Dust affects the biogeochemical cycle by delivering the nutrients (e.g., mineral, nitrogen, and phosphorus) from dust sources to the oceans/other continents (Jickells et al., 2005; Mahowald et al., 2011). Dust aerosol is also one of the main contributors to air pollution that is hazardous to human health (Bell et al., 2008; Lin et al., 2012).

To quantify the dust impacts on Earth system, dust cycle including dust emission, transport, and dry and wet deposition has been incorporated in climate models and Earth System Models (ESMs) since 1990s. These models have the capability to reproduce the general patterns of global dust distribution (e.g., Ginoux et al., 2001; Zender et al., 2003; Yue et al., 2009; Huneeus et al., 2011; Liu et al., 2012b). However, large uncertainties still exist in the simulated global dust budgets in these models, as revealed by a wide range of model results. A comparison of 14 different models from the Aerosol Comparison between Observations and Models (AeroCom) Phase I showed the estimated global dust emission ranges from 514 to 4313 Tg yr^{-1} and annual mean dust burden from 6.8 to 29.5 Tg (Huneeus et al., 2011). Compared to the observations, these models from AeroCom Phase I produce the dust deposition and surface concentration mostly within a

https://doi.org/10.5194/acp-2020-179
Preprint. Discussion started: 3 April 2020

factor of 10 (Huneeus et al., 2011). Uncertainties of dust cycle have led to difficulty in the interpretation of climate impacts of dust aerosol (Yue et al., 2010; Forster et al., 2007; Boucher et al., 2013).

The Coupled Model Intercomparison Project Phase 5 (CMIP5) provides a comprehensive dataset of meteorological variables and climate forcing agents such as aerosols including dust during the period of 1850s to 2000s from a variety of climate models and ESMs. Dust cycle is interactively calculated in some CMIP5 models for historical climate simulations and future climate projections. Till now, only a few studies have investigated dust simulations in CMIP5. Evan et al. (2014) evaluated African dust in 23 CMIP5 models and found the models underestimate dust emission, deposition, and aerosol optical depth (AOD) and have low ability in reproducing the interannual variations of dust burden. Pu and Ginoux (2018) compared the dust optical depth (DOD) from 7 CMIP5 models with satellite observations from 2004 to 2016. They found that these models can capture the global spatial patterns of DOD but with an underestimation of DOD by 25.2% in the boreal spring, and some models cannot capture the seasonal variations of DOD in several key regions such as Northern China and Australia. Wu et al. (2018b) evaluated the dust emission in East Asia from 15 CMIP5 models and found that none of the models can reproduce the observed decline trend of dust event frequency from 1961 to 2005 over East Asia.

None of the above studies has investigated the global dust cycles including their sources and sinks in the CMIP5 models. Therefore, this study is aimed at filling the gap by presenting the strengths and weaknesses of CMIP5 models in simulating global dust cycles. This study will also investigate the associated model uncertainties. As there are a

https://doi.org/10.5194/acp-2020-179
Preprint. Discussion started: 3 April 2020

variety of complexities in the CMIP5 models (Flato et al., 2013), this study aims at identifying the difference in simulated dust cycle as a result of these different complexities. Of particular interest is that some models couple dust emission with dynamic vegetation while the others calculate dust emission based on prescribed vegetation conditions (Table 1), and thus the impacts of dynamic vegetation on dust emission can be examined by comparing the results from these two group models, which has been rarely studied previously.

The paper is organized as follows. Section 2 introduces the CMIP5 models, including the dust emission parameterization. Section 3 describes the observation data used for model validation. Section 4 presents the global dust budget and dust emission, followed by evaluations of dust deposition flux and dust concentration with observations. Discussion and conclusions are given in section 5.

2. Model data

Here we use the historical simulations from 15 CMIP5 models (Table 1). All the 15 models are fully-coupled models used for historical climate simulations and future climate projections, which are included in the Fifth Assessment Report of Intergovernmental Panel on Climate Change (Flato et al., 2013). A brief description of these model is given in Table 1 and more detailed information can be found in the references as listed.

An essential part of dust cycle is dust emission. The dust emission schemes used in these models and the references are also listed in Table 1. Here we only provide a brief summary of similarities and differences in these dust emission schemes. More details can

https://doi.org/10.5194/acp-2020-179
Preprint. Discussion started: 3 April 2020

Atmospheric Chemistry and Physics Discussions

be found in the references (Cakmur et al., 2006; Ginoux et al., 2001, 2004; Marticorena & Bergametti, 1995; Miller et al., 2006; Shao et al., 1996; Takemura et al., 2000, 2009; Tanaka & Chiba, 2005, 2006; Woodward, 2001, 2011; Zender et al., 2003). In general, these emission schemes similarly calculate dust emission based on near-surface wind velocity (in terms of friction wind velocity or wind velocity at 10 m), soil wetness and vegetation cover, and they mainly differ in how to account for these factors and associated input parameters. Particularly, dust emission scheme is coupled to dynamic vegetation in 5 models (GFDL-CM3, HadGEM2-CC, HadGEM2-ES, MIROC-ESM, MIROC-ESM-CHEM). These models use prognostic vegetation to determine the dust source regions. This introduces additional degrees of freedom and thus increases the difficulty in simulating dust emission in these models compared to other models with prescribed vegetation that is constructed from the observation. This will be discussed in Section 4.

Another difference in dust emission scheme is the treatment of dust sizes including the size range and mass partitioning in different sizes. 7 models (GFDL-CM3, MIROC4h, MIROC5, MIROC-ESM, MIROC-ESM-CHEM, MRI-CGCM3, MRI-ESM1) have the same dust size range of 0.2-20 μm in diameter. 5 of the other eight models (CanESM2, CESM1-CAM5, CSIRO-Mk3-6-0, GISS-E2-H, GISS-E2-R) have smaller size ranges (listed in Table 1), while the remaining 3 models (ACCESS1-0, HadGEM2-CC, HadGEM2-ES) have the larger size range of 0.0632-63.2 μm. The impacts of dust size distribution on the simulation of dust cycle will be discussed in later sections. However, as only the total dust emission, deposition, and concentration are provided, we are unable to investigate the difference in the mass partitioning among different dust sizes and its

https://doi.org/10.5194/acp-2020-179
Preprint. Discussion started: 3 April 2020

evolution, which will be left for future studies.

Note that we select these models because they calculate dust emission interactively by their dust emission schemes implemented, and meanwhile, model output of dust emission flux and dust concentration are available from the CMIP5 archive. Also note that not all the models have both dry and wet deposition archived and 8 models provide only dry (GFDL-CM3) or wet deposition flux (CSIRO-Mk3-6-0, HadGEM2-CC, HadGEM2-ES, MIROC4h, MIROC5, MIROC-ESM, MIROC-ESM-CHEM). Therefore, for dust deposition, we derive the global total amount of dry (wet) deposition by subtracting wet (dry) deposition from emission if only wet (dry) deposition is available. For comparison with station observations, we will only use seven models with both dry and wet deposition provided. If there are multiple ensemble simulations available for a specific model, we will use the ensemble means from these simulations for this model (Table 1). The historical simulations of CMIP5 cover the period of 1850-2005. However, some model results prior to 1960 or 1950 are not provided in the CMIP5 archive (e.g., ensemble #2 and #3 from HadGEM2-CC prior to 1960 is not available; MIROC4h prior to 1950 is not available). Therefore, we will focus on the period of 1960-2005 to include as many models as possible and to include as many years as possible for the analysis of present-day dust cycle.

To evaluate the CMIP5 model results, we also use the Modern-Era Retrospective Analysis for Research and Applications, version 2 (MERRA-2). MERRA-2 is the latest atmospheric reanalysis produced by NASA's Global Modeling and Assimilation Office (Gelaro et al., 2017). MERRA-2 assimilates more observation types and have improved significantly compared to its processor, MERRA. A major advancement of MERRA-2 is

https://doi.org/10.5194/acp-2020-179
Preprint. Discussion started: 3 April 2020

that it includes the assimilation of AOD (Randles et al., 2017), which is not included in MERRA and other commonly-used reanalysis datasets such as ECWMF Reanalysis (ERA5) and NCEP/DOE Reanalysis II (R2). The aerosol fields (including dust) in MERRA-2 are significantly improved compared to an identical control simulation that does not include the AOD assimilation (Randles et al., 2017; Buchard et al., 2017). It should be noted that as only AOD is taken into account in the aerosol assimilation, there may be discrepancies in the related aerosol fields such as aerosol concentration and deposition. In addition, dust emission is calculated directly from surface wind speed and soil wetness based on the dust emission scheme of Ginoux et al. (2001), and there is no direct impact on emission from aerosol assimilation. Therefore, there may be inconsistence between dust emission, burden, and deposition. In fact, as shown in the Section 4, there is imbalance between total dust emission and deposition globally and adjustment of dust emission to fit the dust burden is still needed. Despite the limitation, MERRA-2 provides a well-constrained global dust dataset, which is very useful for model evaluations. We will use MERRA-2 as a referential data but with the knowledge of its limitation. We will use the long-term means of dust-related variables during the whole period when data is available (i.e., 1980-2018). Dust in MERRA-2 is treated by five size bins spanning from 0.2 to 20 μm, which are summed to provide the total values. MERRA-2 is provided at the resolution of 0.5º×0.625º, which is similar to one CMIP5 model (MIROC4h) and finer than other CMIP5 models.

3. Observations

There are limited observational datasets that can be used for model evaluations. There is no direct observation of dust emission flux, but satellite observations can provide the locations of dust source regions where dust appears most frequently (e.g., Prospero et al., 2002; Ginoux et al., 2012). Here we do not directly use these observations as they are not available for our usage, but we will refer to the dust source map based on satellite observations from previous studies (e.g., Prospero et al., 2002; Ginoux et al., 2012) and qualitatively compare simulated dust emission regions with them.

Dust deposition is an important constraint on the global dust budget. Here we use the dust deposition flux at 84 stations across the globe available from the AeroCom project (Huneeus et al., 2011). The dataset is compiled from the Dust Indicators and Records in Terrestrial and Marine Paleoenvironments (DIRTMAP) database (Kohfeld and Harrison, 2001) and the data of Ginoux et al., (2001) and Mahowald et al. (1999, 2009). Dust deposition flux are recorded over a period of several to hundreds of years at these stations. There are two types of deposition, dry deposition and wet deposition. To evaluate the contribution of wet deposition to total deposition, we also use the fraction of wet deposition to total deposition at 10 stations, which is compiled by Mahowald et al. (2011). The fraction of wet deposition is obtained from the observations over several years. Note as only minimum and maximum values of fraction of wet deposition are provided for some stations, the average of the minimum and maximum values will be plotted with the range provided when compared with the simulations.

Dust concentration is a key variable that reflects both the dust emission and transport. We use the monthly surface dust concentrations at 20 sites managed by the Rosenstiel School of Marine and Atmospheric Science at the University of Miami

https://doi.org/10.5194/acp-2020-179
Preprint. Discussion started: 3 April 2020

(Prospero, 1996). We also use the monthly surface dust concentrations measured at 2 other stations: Rukomechi, Zimbabwe (Maenhaut et al., 2000a; Nyanganyura et al., 2007) and Jabiru, Australia (Maenhaut et al., 2000b; Vanderzalm et al., 2003). In total, there are 22 stations globally. These stations are generally located in the downwind of dust source regions and some of them are located in the remote regions (Table 2; Figure 1). Measurements at these stations are taken over a period of two to tens of years. This dataset has been widely used to evaluate global dust models (e.g., Ginoux et al., 2001; Zender et al., 2003; Liu et al., 2012b) and also included in the AeroCom project (Huneeus et al., 2011).

We consider the dataset above as a climatology although some of them did not cover a long enough period such as tens of years. The distribution of these stations (for dust deposition, fraction of wet deposition, surface dust concentration) are shown in Figure 1. To compare model results with station observations, bi-linear interpolation is used to generate the model results at the stations.

4. Results

4.1 Global dust budget

First, we present the global dust budgets in CMIP5 models. Table 3 lists the global dust emission, wet deposition, burden, and lifetime in all the 15 models. The area fraction of global dust emissions and ratio of wet deposition to total deposition are also given. Overall, the models estimate the global dust emission in the range of 735-8196 Tg yr^{-1}, with the MIROC4h having the lowest and two Hadley models (HadGEM2-CC and HadGEM2-ES) having the highest emissions. The global dust emissions in CMIP5 models differ by about 11 times compared to about 8 times in the AeroCom models, which give dust emissions in the range of 514-4313 Tg yr^{-1} (Huneeus et al., 2011). This can be ascribed to a larger difference in the complexity of CMIP5 models compared to AeroCom models (Section 2). In particular, HadGEM2-CC and HadGEM2-ES give about twice of the largest emission estimated in the AeroCom models. The larger value in HadGEM2-CC and HadGEM2-ES is mainly due to the overestimation of bare soil area by the dynamic vegetation module in these models (Collins et al., 2011; Martin et al., 2011). Additionally, the larger value may be also related to the larger dust size range in the models (0.06 to 63 μm) with about 3300 Tg yr^{-1} of dust emission for particles smaller than 20 μm diameter (Bellouin et al, 2011). However, ACCESS1.0 with the same size range as HadGEM2-CC and HadGEM2-ES produces 3-4 times smaller dust mission. As shown in the evaluation of surface dust concentrations in Section 4.4, HadGEM2-CC and HadGEM2-ES consistently overestimate the surface dust concentrations at the selected stations (by 5 times on average). The MIROC4h model underestimates the surface dust concentrations by more than 10 times (Section 4.4). If the estimations of MIROC4h, HadGEM2-CC and HadGEM2-ES are not considered, global dust emissions in CMIP5 models are in the range of 1246-3698 Tg yr^{-1}, comparable to AeroCom results (Huneeus et al., 2011) and other estimations (e.g., Shao et al., 2011). The global dust emission in MERRA-2 is 1620 Tg yr^{-1}, which is within the range of CMIP5 models.

For dust deposition, dust particles are deposited to the Earth's surface mainly by dry deposition, and wet deposition accounts for 12-39% of total deposition in CMIP5 models. The ratio of wet deposition to total deposition depends on several factors, for example, dust size distribution, geographical locations of dust emission regions, and climate states

https://doi.org/10.5194/acp-2020-179
Preprint. Discussion started: 3 April 2020

such as circulation and precipitation (e.g., Wu and Lin, 2013). The estimated global dust burden ranges from 2.5 to 41.9 Tg, and from 8.1 to 36.1 Tg when MIROC4h and HadGEM2-CC/ES are excluded. The lifetime of global dust particles ranges from 1.3 to 4.4 days. The dust burden (lifetime) in MERRA-2 is 20.3 Tg (4.1 days), which is larger (longer) than most CMIP5 models. The fraction of wet deposition to total deposition in MERRA-2 is 38.6%, which is in the upper end of CMIP5 results. There is a linear relationship (with the correlation coefficient R=0.67, above the statistically significant level of 0.01) between global dust burden and lifetime in CMIP5 models (excluding HadGEM2-CC/ES; Figure 2a), indicating a longer lifetime of dust is generally associated with a larger dust burden. Linear relationship (R=0.46, above the statistically significant level of 0.05) is also found between lifetime and fraction of wet deposition (Figure 2b), which indicates that a longer lifetime corresponds to a larger fraction of wet deposition in the total deposition.

4.2 Global dust emissions

Dust emission is the first and the foremost process in the dust cycle and determines the amount of dust entrained into the atmosphere. Figure 3 shows the spatial distribution of dust emission fluxes from 15 CMIP5 models and MERRA-2 reanalysis. In general, all the models can reproduce the main dust sources, known as the “dust belt” that extends from North Africa, Middle East, Central Asia, South Asia, to East Asia and that can be seen from satellite observations (Prospero et al., 2002; Ginoux et al., 2012). However, the models differ significantly in the extent of this “dust belt”. Although a large group of CMIP5 models (CSIRO-Mk3-6-0, GFDL-CM3, GISS-E2-H/S, MIROC5, MIROC-ESM,

https://doi.org/10.5194/acp-2020-179
Preprint. Discussion started: 3 April 2020

MIROC-ESM-CHEM, MRI-CGCM3, and MRI-ESM1) simulate similarly the dust emission regions mostly over deserts and adjacent arid/semi-arid regions, two of the models (CESM1-CAM5 and MIROC4h) simulate much smaller areas of dust emission and a few others (ACCESS1-0, CanESM2, HadGEM2-CC/ES) simulate more extended dust emission regions. CESM1-CAM5 simulates isolated dust emission regions with "hot spots" of dust emissions larger than 500 g m^{-2} yr^{-1}, and dust emission in MIROC4h concentrates only over the centers of deserts. In contrast, ACCESS1-0, CanESM2, and HadGEM2-CC/ES not only simulate the dust emissions in deserts and adjacent regions, but also produce a considerable amount of dust emissions over the Eastern Africa (Somalia, Ethiopia, and Kenya), East India, and northern part of Indo China Peninsula, which are rarely regarded as potential dust sources (Formenti et al., 2011; Shao, 2008).

Dust sources also exist in Australia, North America, South America, and South Africa, as evident from surface observations (e.g., Shao, 2008) and satellite observations (Prospero et al., 2002; Ginoux et al., 2012), although the emission fluxes are smaller than those in the aforementioned "dust belt". In these regions, most models produce a considerable amount of dust emissions (>5 g m^{-2} yr^{-1}), while a small group of models simulate much less or even negligible dust emissions. The models differ greatly in these regions. For example, in Australia, two models (MIROC-ESM and MIROC-ESM-CHEM) produces little dust emissions, while seven models (ACCESS1-0, CanESM2, CSIRO-Mk3-6-0, GISS-E2-H/R, HadGEM2-CC/ES) produce much larger dust emissions with emission fluxes higher than 10 g m^{-2} yr^{-1} in a large part of the region. In North America which also has some dust sources (Wu et al., 2018a), five models (MIROC4h, MIROC-ESM, MIROC-ESM-CHEM, MRI-CGCM3, MRI-ESM1) simulate little dust emissions,

https://doi.org/10.5194/acp-2020-179
Preprint. Discussion started: 3 April 2020

while four models (ACCESS1-0, CanESM2, HadGEM2-CC/ES) simulate dust emission fluxes exceeding 5 g m^{-2} yr^{-1} in a large part of the region. Note that ACCESS1-0 and CanESMs also produce dust emissions in the high latitudes of Northern Hemisphere (>60 ºN) and eastern part of South America. The importance of high latitude dust is recognized recently (Bullard et al., 2016), but the eastern part of South America has not been regarded as a potential dust source (Formenti et al., 2011; Shao, 2008).

The contributions of dust emissions in nine different regions to global dust emission is summarized in Table 4. The models consistently simulate the largest dust emission in North Africa, which accounts for 36-79% of the global total dust emission. The models also estimate large dust emissions in Middle East and East Asia, which account for 7-20% and 4-19% of global dust emission, respectively. The contributions from Central Asia and South Asia in CMIP5 models range from 1-14% and 0.9-10%, respectively. The contributions from other sources (North America, South Africa, Australia, South America) are much less consistent among the models, and the largest difference is in North America (0.008-4.5%) and Australia (0.02-28%) by three orders of magnitude.

Particularly, HadGEM2-CC/ES simulate 25-28% of global dust emission from Australia, which is comparable to that from sum of all Asian sources (Middle East, Central Asia, South Asia, and East Asia). This estimate is unrealistically high, as will be indicated by the comparison of surface dust concentrations in Section 4.4. The excessive dust emission in Australia from HadGEM2-CC/ES may be related to the prognostic vegetation used for dust emission, as the ACCESS1-0 model that uses the similar dust emission parameterization but with the prescribed vegetation simulates a much lower dust emission. The lowest dust emission in Australia is simulated by MIROC-ESM and

MIROC-ESM-CHEM, which contribute only 0.02-0.03% (1 Tg yr^{-1} or less) to the total dust emission . This estimate is unrealistically low as Australia is an important dust source (e.g., Shao et al., 2007) and is also much smaller than previous studies (e.g., Hunuees et al., 2011). The low dust emission in Australia from MIROC-ESM and MIROC-ESM-CHEM may be related to the prognostic vegetation used for dust emission, as the two other MIROC family models (MIROC4h and MIROC5) simulate significantly higher dust emissions (~1% of total dust emission).

The contributions from nine source regions in MERRA-2 to the total dust emission are within the range of CMIP5 models. MERRA-2 estimates are obtained through the assimilation of meteorology in model integrations and therefore uncertainties are reduced.

Since the amount of global dust emission differs substantially among different models, the dust emission flux is further normalized by its global mean value in each model for the comparison of dust emission area and intensity (Figure 4). Here the dust emission area is defined as the region with normalized emission flux greater than 0.01. Among the CMIP5 models, CESM-CAM5 and MIROC4h simulate the smallest dust emission area, which are 2-3% of the global surface area, while CanESM2 simulates the largest dust emission area (18% of the global surface area; Figure 4 and Table 3). The maximum normalized dust emission flux is also the largest at 2682 and 3635 in CESM1-CAM5 and MIROC4h, respectively, indicating the “hot spots” with extremely high dust emission flux in the two models. The maximum normalized dust emission flux is generally between 100 and 300 in other CMIP5 models and is approximately 200 in MERRA-2 reanalysis.

The smallest dust emission area in CESM1-CAM5 is mainly because the model adopts a geomorphic source erodibility with a threshold value of 0.1 for the dust emission occurrences (Zender et al., 2003; Wu et al., 2016). Small dust emission area in MIROC4h may be partly due to the higher horizontal resolution of the model (0.56º) than other models (1º-3º) including MIROC5 (Table 1). The higher model resolution may change the patterns of wind speeds and precipitation as well as the occurrence frequency of strong winds and heavy precipitation and thus affect the dust emission regions. The largest dust emission area in CanESM2 may be due to its prescribed land cover map, and/or adoption of gustiness adjustment for wind friction velocity (von Salzen et al., 2013). MERRA-2 gives a value of 7.4% for the dust emission area, which is in the median of all the CMIP5 model results.

As normalized dust emission flux is comparable among the CMIP5 models, a global map of multi-model mean and standard deviation of normalized dust emission flux are thus constructed and shown in Figure 5. The multi-model mean represents the general consensus among the CMIP5 models while the standard deviation indicates the variability among models. The relative standard deviation is calculated by the ratio of standard deviation to the mean, which is shown to illustrate the uncertainty among the models. Mean normalized dust emission flux is large (>10) in the desert regions in North Africa, Middle East, Central Asia, South Asia, East Asia, and Australia (Figure 5a). It ranges from 1-10 in the desert adjacent regions and in small regions of South America, North America, and South Africa (Figure 5a). The patterns of standard deviation of multi-model results are generally similar to those of mean normalized dust emission flux (Figure 5b). However, the relative standard deviation is quite different from the mean normalized dust emission flux, and its pattern is nearly opposite (Figure 5c). The relative standard deviation is mostly below 1 in the aforementioned desert regions with larger mean normalized dust emission (>10) and increases to 1-4 in other regions with relative smaller dust emission, indicating the large uncertainty of estimated dust emission flux in the CMIP5 models.

Difference of dust emission uncertainty in different regions can be explained by two reasons. First, in the deserts, soil is extremely dry (below the criteria for dust emission) and surface is covered with little vegetation. In these regions, the models agree with each other more easily in simulating the occurrence of dust emission. In the regions adjacent to the deserts or with localized sandy lands, where soil is wetter and there is more vegetation cover at the surface, the models differ significantly in the parameterizations of dust emission, treatment of land cover, and simulated meteorology, and thus climate models differ in their estimation of dust emission more strongly. Second, there are a larger variety of complexities in the CMIP5 models compared to the models participating in the AeroCom intercomparison (Section 2). Some models use the dynamic vegetation for dust emission (e.g., HadGEM2-CC/ES, MIROC-ESM, MIROC-ESM-CHEM), and deviate largely from other models over the regions with sparse vegetation cover such as Australia. This further increases the differences in dust emission among the CMIP5 models.

4.3 Dust deposition flux

Dust deposition is a vital process in the dust cycle which removes dust particles from the atmosphere and provides nutrients to the terrestrial and marine ecosystems.

https://doi.org/10.5194/acp-2020-179
Preprint. Discussion started: 3 April 2020

Figure 6 shows the comparison of dust deposition flux at 84 selected stations between the models and observations. Only seven CMIP5 models provide total dust deposition flux (sum of dry and wet deposition), which are used here. The global dust emission in these seven models ranges from 1600 to 3500 Tg yr^{-1}, which is at the medium level of all the CMIP5 models. Observed annual mean dust deposition flux ranges from 10^{-4} to 10^{3} g m^{-2} yr^{-1}, indicating large spatial variabilities of dust deposition. In general, six of seven CMIP5 models (excluding ACCESS1-0) reproduces the observed dust deposition flux within a factor of 10 in most regions except over the Southern Ocean, Antarctica, and Pacific. Over the Southern Ocean and in the Antarctica, all the models except CESM1-CAM5 overestimate the dust deposition flux by more than a factor of 10 at two stations. Over the Pacific Ocean, all the models except CanESM2 underestimate the dust deposition flux by more than 10 times at several stations. In addition to the overestimation over the Southern Ocean and Antarctica and the underestimation over the Pacific Ocean, ACCESS1-0 mostly underestimate the dust deposition flux in other regions with underestimation by more than a factor of 10 at several stations. Overall ACCESS1-0 underestimates the dust deposition flux by approximately a factor of 2 on average.

Similar to most of the CMIP5 models, MERRA-2 reproduces the observed dust deposition flux within a factor of 10 at most stations except over the Southern Ocean and Antarctica. Over the Southern Ocean and Antarctica, MERRA-2 tends to overestimate the dust deposition flux by more than a factor of 10 at most stations. Compared to the CMIP5 models, larger dust deposition over the Southern Ocean and Antarctica in MERRA-2 may be related to the adoption of both meteorology and aerosol assimilation

https://doi.org/10.5194/acp-2020-179
Preprint. Discussion started: 3 April 2020

in MERRA-2, which affects the dust transport and deposition. As mentioned in Section 2, only AOD is taken into account in the aerosol assimilation for MERRA-2. Therefore the large discrepancy of dust deposition at several stations in MERRA-2 may result from the unrealistic representation of dust vertical profiles, size distribution, and deposition process. Overall, the correlation coefficients between CMIP5 models and observations (after taking the logarithms of both them; R_{log}) range from 0.90 to 0.92 and are slightly higher than that of MERRA-2 (0.87).

Dust deposition includes two mechanisms: dry and wet deposition. Figure 7 shows the comparison of fraction of wet deposition in total deposition from models and observations at 10 stations. These stations are located downwind of dust sources and can be classified into two groups. One group are Bermuda (station #1) over the western Atlantic Ocean, Amsterdam Island (station #2) over the southern Indian Ocean, Cape Ferrat (station #3) in southern Europe, and New Zealand (station #6). For this group of stations, fractions of wet deposition range from 17% to 70%. At these stations, all the models simulate the fractions of wet deposition exceeding 75% and significantly overestimate the fractions of wet deposition. MERRA-2 estimates smaller fractions of wet deposition compared to the CMIP5 models but still significantly overestimates fractions of wet deposition at these stations.

The other group includes Enewetak Atoll (station #4), Samoa (station #5) and Fanning (station #8) over the tropical Pacific Ocean, Midway (station #7) over the subtropical Pacific Ocean, Greenland (station #9) and Coastal Antarctica (station #10) in the high latitudes. These stations are thousands of kilometers away from sources. At these stations, observed fractions of wet deposition range from 65% to 90%, indicating the dominance of wet deposition. Most of CMIP5 models except CanESM2 simulate the fractions of wet deposition within 20% of observations. CanESM2 also simulates the fraction of wet deposition comparable to observations except at Coastal Antarctica where CanESM2 underestimates the fraction of wet deposition by up to 35%. MERRA-2 captures well the fraction of wet deposition over the tropical and subtropical Pacific Ocean but significantly underestimate it by 40-45% in the high latitudes. The large underestimation by CanESM2 and MERRA-2 may be related to the meteorology such as precipitation and turbulent flux, or the parameterizations of dust deposition in the models, which deserves future investigations.

Dust cycle can deliver nutrients from continents to oceans. Table 5 summarizes the dust deposition and fraction of wet deposition onto the global surface, continents and oceans, respectively in seven CMIP5 models and MERRA-2 reanalysis. Total deposition in continents ranges from 1331 to 2850 Tg yr^{-1} in seven CMIP5 models and accounts for 77-91 % of global total deposition. Total deposition in all the oceans ranges from 197 to 686 Tg yr^{-1} and accounts for 9-23 % of global total deposition, indicating a considerable uncertainty in dust deposition, which should be taken into account in modeling the marine biogeochemistry with ESMs. MERRA-2 estimates 71% (29%) of dust deposited in continents (oceans), and this estimation is smaller (larger) than all seven CMIP5 models, indicating MERRA-2 transport dust more efficiently to oceans. This is consistent with the comparison of dust deposition flux shown in Figure 6 and may be related to the assimilation of both meteorology and aerosols in MERRA-2. The fractions of wet deposition (with respect to total deposition) in seven CMIP5 models are 8-33% and 49-71% over continents and oceans, respectively. MERRA-2 estimates the fraction of wet deposition (with respect to total deposition) 26% and 69% over the continents and oceans, respectively, which lie within the range of CMIP5 models.

4.4 Dust concentration

Dust concentration is an important variable for its cycle. Figure 8 shows the comparison of surface dust concentrations between models and observations at 22 selected stations. These stations are located in the downwind regions of dust sources, and annual mean dust concentrations at these stations range from 10^{-1} to 10^{2} μg m^{-3}. In general, the models reproduce observed surface dust concentrations within a factor of 10, with the exceptions of HadGEM2-CC/ES and MIROC4h. Although HadGEM2-CC/ES simulate well observed surface dust concentrations at the stations over the Atlantic Ocean (stations #1-4) and slightly underestimate the observations in East Asia (stations #7-8), the two models significantly overestimate surface dust concentrations at most of other stations especially at the station located in Australia and downwind regions (stations #15-21). This is consistent with their much higher dust emission in Australia compared to other models (Table 3; Section 4.2). In contrast, MIROC4h largely underestimates surface dust concentrations by 1-2 orders of magnitude at most stations. Although compared to MIROC5, MIROC4h only simulates approximately 4 times lower global dust emission, MIROC4h tends to concentrate all the dust emissions over smaller regions of global surface (2.9% compared to 6.1%). Therefore, dust is less widely distributed in the atmosphere and a smaller fraction of dust is transported to the downwind regions in MIROC4h, as indicated by its almost 8 times smaller dust burden and only half the dust

https://doi.org/10.5194/acp-2020-179
Preprint. Discussion started: 3 April 2020

lifetime compared to MIROC5. This difference can explain lower surface dust concentrations in MIROC4h.

Although the CMIP5 models (excluding MIROC4h and HadGEM2-CC/ES) can roughly reproduce the observed magnitudes of surface dust concentrations at most stations, considerable discrepancy between models and observations can be found at certain regions. Most models except CanESM2 significantly underestimate dust concentrations at stations in Antarctica (stations #21 and #22), with the largest underestimation by more than 2 orders of magnitude in MIROC-ESM/MIROC-ESM-CHEM which also simulates much lower dust emissions in Australia, South Africa, and southeastern South America. Eight models (ACCESS1-0, CESM-CAM5, CSIRO-Mk3-6-0, GFDL-CM3, GISS-E2-H/R, MRI-CGCM3, MRI-ESM1) largely underestimate dust concentrations by 1-2 orders of magnitude at station #6 in South Africa. Three MIROC family models (MOROC5, MOROC-ESM, MIROC-ESM-CHEM) underestimate dust concentrations by 1-2 orders of magnitude at several stations in the downwind regions of Australia (stations #14, 15, and 17). Other noticeable discrepancies include underestimations in East Asia by ACCES1-0/MIROC5, underestimations over the Tropical Pacific Ocean by CESM-CAM5/GISS-H2-H/GISS-E2-R, and overestimations in Australia by CanESM2.

Overall the correlation coefficients and mean biases between CMIP5 models and observations (after taking the logarithms of both of them; R_{log} and MB_{log}) ranges from 0.55 to 0.88 and from -5.59 to 1.52 for all CMIP5 models, respectively. If HadGEM2-CC/ES and MIORC4h are excluded for the calculation, R_{log} and MB_{log} range from 0.60 to 0.88 and from -1.61 to 1.04, respectively. As a MB_{log} of -0.7 (0.7) corresponds to a

https://doi.org/10.5194/acp-2020-179
Preprint. Discussion started: 3 April 2020

Atmospheric Chemistry and Physics Discussions

general underestimation (overestimation) by a factor of 2, six models (CESM1-CAM5, GISS-E2-H/R, MIROC5, MIROC-ESM, MIROC-ESM-CHEM) underestimate surface dust concentrations by more than a factor of 2 on average, while CanESM2 overestimates surface dust concentrations by the similar magnitude.

Compared to observations, MERRA-2 simulates well the dust concentrations at all stations except station #6 in South Africa. This improvement by MERRA-2 compared to the CMIP5 models may be due to the inclusion of both meteorology and aerosol assimilation in MERRA-2. The correlation coefficients (R_{log}) between MERRA-2 and observations is 0.91, which is larger than all the CMIP5 models, and mean bias (MB_{log}) is close to zero (0.01).

5. Discussion and Conclusions

In this study we examine the present-day global dust cycle simulated by the 15 climate models participating in the CMIP5 project. The simulations are also compared with a dataset MERRA-2 and observations of dust deposition and concentration. The results show that the global dust emission in these models ranges from 735 to 8186 Tg yr^{-1} and the global dust burden ranges from 2.5 to 41.9 Tg. The differences are larger than those from models participating in the AeroCom project (Huneeus et al., 2011), which is a result of enhanced model complexities in modeling both climate and dust emission in the CMIP5 models.

The simulated dust emission regions also differ greatly accounting for a global surface area of 2.9%-18%. The models agree most with each other in reproducing the "dust belt" that extends from North Africa, Middle East, Central Asia, South Asia, to East

https://doi.org/10.5194/acp-2020-179
Preprint. Discussion started: 3 April 2020

Asia, but there are large uncertainties in the extent of this "dust belt" and other source regions including Australia, North America, South America, and South Africa. Particularly, some models simulate little dust emissions (<0.1% of global dust emission) in Australia and North America, while some other models simulate larger dust emissions there which account for 10-30% and 3-4% of global dust emission in Australia and North America, respectively. It is also revealed that the increasing complexity of ESMs (HadGEM2-CC/ES, MIROC-ESM, and MIROC-ESM-CHEM) by coupling dust emission with dynamic vegetation can amplify the uncertainty associated with dust emissions.

Removal of dust particles in the CMIP5 models is mainly through dry deposition, and wet deposition only accounts for 12-39% of total deposition. The associated dust life time is about 1.3-4.4 days. A clear linear relationship between dust burden, dust lifetime, and fraction of wet deposition to total deposition is present in the CMIP5 models, suggesting a general consistency among these models. The models also estimate that 77-91% of emitted dust are deposited back to continents and 9-23% of them are deposited to the oceans. The fraction of wet deposition is smaller in most CMIP5 models and dust lifetime is shorter compared to MERRA-2 reanalysis, indicating a shorter distance for dust transport from its sources in most CMIP5 models. Compared to the observations, the CMIP5 models (except MIRCO4h) reproduce dust deposition flux and surface dust concentration by a factor of 10 at most stations. Larger discrepancies are found in the remote regions such as Antarctica and Tropical Pacific Ocean. In Australia and downwind regions, four MIROC family models (MIROC4h, MIROC5, MIROC-ESM, MIROC-ESM-CHEM) which simulate little dust emission in Australia largely

https://doi.org/10.5194/acp-2020-179
Preprint. Discussion started: 3 April 2020

Atmospheric Chemistry and Physics Discussions

underestimate the dust concentrations at stations in the remote regions. Contrarily HadGEM2-CC/ES overestimate dust concentrations. MIROC4h shows the largest discrepancy by underestimating the surface dust concentrations by more than a factor of 100 in Australia and downwind regions. Overall, although MIROC4h simulates 4-5 times lower global dust emission than other three MIROC family models, MIROC4h simulates on average more than 50 times smaller surface dust concentrations at 22 stations. This can be ascribed to the fact that most dust emissions in MIROC4h are concentrated over the desert centers, which limits the long-range transport of dust particles to the remote regions.

These results show large uncertainties of global dust cycle in ESMs. In fact, these models are fully-coupled atmosphere-land-ocean models and some of them also include the dynamic vegetation. As a result, uncertainties are larger compared to those in previous models participating in the AeroCom intercomparison project where sea surface temperature is prescribed, and more strictly, in some models, meteorological fields are prescribed from reanalysis (Huneeus et al., 2011). Larger uncertainties in the CMIP5 models with dynamic vegetation is expected, as a prognostic vegetation would depart from the observed or constructed vegetation and may also lead to a large bias in soil moisture, which may thus lead to an additional bias in dust emissions in these models. Uncertainties of dust simulations also vary with regions, and a smaller uncertainty is found in the deserts over the "dust belt" in the North Hemisphere, but a larger uncertainty exists in other regions including Australia and North America. The large uncertainties of global dust cycle in the CMIP5 models would cast a doubt on the reliability of dust radiative forcing estimated in these models.

Because the dust lifecycle involves various processes with the scales from micrometers to tens of thousands of kilometers and consists of lots of parameters, the representation of dust cycle in climate models is a big challenge for the model community. Dust emission is the first and foremost process for model improvements of dust cycle (Shao, 2008; Shao et al., 2011). Improving dust emission not only lies in the development of dust emission scheme but also in its implementation into climate models (e.g., Shao, 2008; Wu et al., 2016; Wu et al., 2019). For example, different dust emission schemes with specific land cover datasets and criteria for the occurrence of dust emission are adopted in the models (Table 1 and references therein). Therefore, different results of dust emission among the CMIP5 models reflect in many aspects the differences in meteorology, land cover data, and dust emission parameterizations. A close look at these factors in each model will help to unravel reasons behind the biases in these models. In addition, the models are only evaluated with observed dust deposition and surface concentrations. Although it is roughly acceptable, it is also desirable to collect the observations of dust emission flux and use them for model evaluation. Particularly, for dust deposition and dust concentration, some biases come from dust emission and others from circulation and deposition parameterizations. It is only possible to separate the contributions of different processes to the biases in dust deposition and concentration, if observations of dust emission are also included in model comparison.

It should be mentioned that dust size distribution is an important parameter for dust cycle (e.g., Shao, 2008; Mahowald et al., 2014), and it is not included in this study as the model data are not available. Evolution of dust size distribution during dust transport and deposition is critical to our understanding of the model bias in dust cycle. We suggest that

https://doi.org/10.5194/acp-2020-179
Preprint. Discussion started: 3 April 2020

the size-resolved dust emission, concentration, and deposition should be outputted and provided in the latest CMIP6 project (Eyring et al., 2016). Moreover, observations of size-resolved dust concentration and deposition is urgently needed. A compile of available observations of dust size distribution (e.g., Mahowald et al., 2014: Ryder et al., 2018) are also required for model evaluation.

Data availability

CMIP5 results are available in https://esgf-node.llnl.gov/search/cmip5/. MERRA-2 is available in https://disc.gsfc.nasa.gov/datasets?project=MERRA-2. Observations of dust deposition and fraction of wet deposition is provided in the literature led by N. Huneeus (https://www.atmos-chem-phys.net/11/7781/2011/). Observations of surface dust concentrations are provided by Joseph M. Prospero from the Rosenstiel School of Marine and Atmospheric Science at the University of Miami.

Author contributions

CW and ZL designed the study. CW did the data analyses with advices from ZL and XL. CW wrote the manuscript with contributions from ZL and XL.

Competing interests

The authors declare that they have no conflict of interest.

Acknowledgement

This research is jointly supported by the National Natural Science Foundation of

https://doi.org/10.5194/acp-2020-179
Preprint. Discussion started: 3 April 2020

China (grant 41975119 and 41830966), Chinese Academy of Sciences (CAS) Strategic Priority Research Program (grant XDA19030403), and CAS The Belt and Road Initiatives Program on International Cooperation (grant 134111KYSB20060010). C. Wu is supported by the CAS Pioneer Hundred Talents Program for Promising Youth (Class C). We acknowledge the WCRP's Working Group on Coupled Modelling, which is responsible for CMIP, and the various climate modeling groups for producing and making available their model output. We also thank the team for generating MERRA-2 data and make them available. We also thank Prof. Joseph M. Prospero for providing the observations of surface dust concentrations and helpful discussions.

References

Adachi, Y., Yukimoto, S., Deushi, M., Obata, A., Nakano, H., Tanaka, T. Y., et al.: Basic performance of a new earth system model of the Meteorological Research Institute (MRI-ESM 1). Papers in Meteorology and Geophysics, 64, 1-19, https://doi.org/10.2467/mripapers, 2013.

Arora, V. K., Scinocca, J. F., Boer, G. J., Christian, J. R., Denman, K. L., Flato, G. M., Kharin, V. V., Lee, W. G., and Merryfield, W. J.: Carbon emission limits required to satisfy future representative concentration pathways of greenhouse gases, Geophys Res Lett, 38, https://doi.org/10.1029/2010GL046270, 2011.

Bell, M. L., Levy, J. K., and Lin, Z.: The effect of sandstorms and air pollution on cause-specific hospital admissions in Taipei, Taiwan, Occup Environ Med, 65, 104-111, https://doi.org/10.1136/oem.2006.031500, 2008.

Bellouin, N., Rae, J., Jones, A., Johnson, C., Haywood, J., and Boucher, O.: Aerosol forcing in the Climate Model Intercomparison Project (CMIP5) simulations by HadGEM2-ES and the role of ammonium nitrate, 116, https://doi.org/10.1029/2011jd016074, 2011.

Bi, D., Dix, M., Marsland, S., O' Farrell, S., Rashid, H., Uotila, P., et al.: The ACCESS Coupled Model: Description, control climate and evaluation. Australian Meteorological and Oceanographic Journal, 63(1), 41-64, 10.22499/2.6301.004, 2013.

Boucher, O., Randall, D., Artaxo, P., Bretherton, C., Feingold, G., Forster, P., Kerminen,

https://doi.org/10.5194/acp-2020-179
Preprint. Discussion started: 3 April 2020

V.-M., Kondo, Y., Liao, H., and Lohmann, U.: Clouds and aerosols, in: Climate change 2013: the physical science basis. Contribution of Working Group I to the Fifth Assessment Report of the Intergovernmental Panel on Climate Change, Cambridge University Press, 571-657, 2013.

Buchard, V., Randles, C. A., Silva, A. M. d., Darmenov, A., Colarco, P. R., Govindaraju, R., Ferrare, R., Hair, J., Beyersdorf, A. J., Ziemba, L. D., and Yu, H.: The MERRA-2 Aerosol Reanalysis, 1980 Onward. Part II: Evaluation and Case Studies, 30, 6851-6872, https://doi.org/10.1175/jcli-d-16-0613.1, 2017.

Bullard, J. E., Baddock, M., Bradwell, T., Crusius, J., Darlington, E., Gaiero, D., Gassó, S., Gisladottir, G., Hodgkins, R., McCulloch, R., McKenna-Neuman, C., Mockford, T., Stewart, H., and Thorsteinsson, T.: High-latitude dust in the Earth system, 54, 447-485, https://doi.org/10.1002/2016rg000518, 2016.

Cakmur, R. V., Miller, R. L., Perlwitz, J., Geogdzhayev, I. V., Ginoux, P., Koch, D., Kohfeld, K. E., Tegen, I., and Zender, C. S.: Constraining the magnitude of the global dust cycle by minimizing the difference between a model and observations, Journal of Geophysical Research: Atmospheres, 111, https://doi.org/doi:10.1029/2005JD005791, 2006.

Collins, W. J., Bellouin, N., Doutriaux-Boucher, M., Gedney, N., Halloran, P., Hinton, T., Hughes, J., Jones, C. D., Joshi, M., Liddicoat, S., Martin, G., O'Connor, F., Rae, J., Senior, C., Sitch, S., Totterdell, I., Wiltshire, A., and Woodward, S.: Development and evaluation of an Earth-System model – HadGEM2, Geosci. Model Dev., 4, 1051-1075, https://doi.org/10.5194/gmd-4-1051-2011, 2011.

Delworth, T. L., Broccoli, A. J., Rosati, A., Stouffer, R. J., Balaji, V., Beesley, J. A., Cooke, W. F., Dixon, K. W., Dunne, J., Dunne, K. A., Durachta, J. W., Findell, K. L., Ginoux, P., Gnanadesikan, A., Gordon, C. T., Griffies, S. M., Gudgel, R., Harrison, M. J., Held, I. M., Hemler, R. S., Horowitz, L. W., Klein, S. A., Knutson, T. R., Kushner, P. J., Langenhorst, A. R., Lee, H.-C., Lin, S.-J., Lu, J., Malyshev, S. L., Milly, P. C. D., Ramaswamy, V., Russell, J., Schwarzkopf, M. D., Shevliakova, E., Sirutis, J. J., Spelman, M. J., Stern, W. F., Winton, M., Wittenberg, A. T., Wyman, B., Zeng, F., and Zhang, R.: GFDL's CM2 Global Coupled Climate Models. Part I: Formulation and Simulation Characteristics, J Climate, 19, 643-674, https://doi.org/10.1175/jcli3629.1, 2006.

Dix, M., Vohralik, P., Bi, D., Rashid, H., Marsland, S., O' Farrell, S., et al.: The ACCESS Coupled Model: Documentation of core CMIP5 simulations and initial results. Australian Meteorological and Oceanographic Journal, 63(1), 83-99, 10.22499/2.6301.005, 2013.

Donner, L. J., Wyman, B. L., Hemler, R. S., Horowitz, L. W., Ming, Y., Zhao, M., Golaz,

https://doi.org/10.5194/acp-2020-179
Preprint. Discussion started: 3 April 2020

J.-C., Ginoux, P., Lin, S.-J., Schwarzkopf, M. D., Austin, J., Alaka, G., Cooke, W. F., Delworth, T. L., Freidenreich, S. M., Gordon, C. T., Griffies, S. M., Held, I. M., Hurlin, W. J., Klein, S. A., Knutson, T. R., Langenhorst, A. R., Lee, H.-C., Lin, Y., Magi, B. I., Malyshev, S. L., Milly, P. C. D., Naik, V., Nath, M. J., Pincus, R., Ploshay, J. J., Ramaswamy, V., Seman, C. J., Shevliakova, E., Sirutis, J. J., Stern, W. F., Stouffer, R. J., Wilson, R. J., Winton, M., Wittenberg, A. T., and Zeng, F.: The Dynamical Core, Physical Parameterizations, and Basic Simulation Characteristics of the Atmospheric Component AM3 of the GFDL Global Coupled Model CM3, J Climate, 24, 3484-3519, https://doi.org/10.1175/2011jcli3955.1, 2011.

Evan, A. T., Flamant, C., Fiedler, S., and Doherty, O.: An analysis of aeolian dust in climate models, Geophys Res Lett, 41, 5996-6001, 10.1002/2014GL060545, 2014.

Eyring, V., Bony, S., Meehl, G. A., Senior, C. A., Stevens, B., Stouffer, R. J., and Taylor, K. E.: Overview of the Coupled Model Intercomparison Project Phase 6 (CMIP6) experimental design and organization, Geosci. Model Dev., 9, 1937-1958, https://doi.org/10.5194/gmd-9-1937-2016, 2016.

Flato, G., Marotzke, J., Abiodun, B., Braconnot, P., Chou, S.C., Collins, W., Cox, P., Driouech, F., Emori, S., Eyring, V., Forest, C., Gleckler, P., Guilyardi, E., Jakob, C., Kattsov, V., Reason, C. and Rummukainen, M.: Evaluation of Climate Models. In: Climate Change 2013: The Physical Science Basis. Contribution of Working Group I to the Fifth Assessment Report of the Intergovernmental Panel on Climate Change, Cambridge University Press, Cambridge, United Kingdom, 741-866, 2013.

Formenti, P., Schutz, L., Balkanski, Y., Desboeufs, K., Ebert, M., Kandler, K., Petzold, A., Scheuvens, D., Weinbruch, S., and Zhang, D.: Recent progress in understanding physical and chemical properties of African and Asian mineral dust, Atmos Chem Phys, 11, 8231-8256, https://doi.org/10.5194/acp-11-8231-2011, 2011.

Forster, P., et al., Changes in atmospheric constituents and in radiative forcing, in Climate Change 2007: The Physical Science Basis. Contribution of Working Group I to the Fourth Assessment Report of the Intergovernmental Panel on Climate Change, edited by S. Solomon et al., Cambridge Univ. Press, Cambridge, U. K, 129-234, 2007.

Gelaro, R., McCarty, W., Suárez, M. J., Todling, R., Molod, A., Takacs, L., Randles, C. A., Darmenov, A., Bosilovich, M. G., Reichle, R., Wargan, K., Coy, L., Cullather, R., Draper, C., Akella, S., Buchard, V., Conaty, A., Silva, A. M. d., Gu, W., Kim, G.-K., Koster, R., Lucchesi, R., Merkova, D., Nielsen, J. E., Partyka, G., Pawson, S., Putman, W., Rienecker, M., Schubert, S. D., Sienkiewicz, M., and Zhao, B.: The Modern-Era Retrospective Analysis for Research and Applications, Version 2 (MERRA-2), 30, 5419-5454, https://doi.org/10.1175/jcli-d-16-0758.1, 2017.

https://doi.org/10.5194/acp-2020-179
Preprint. Discussion started: 3 April 2020

Ginoux, P., Chin, M., Tegen, I., Prospero, J. M., Holben, B., Dubovik, O., and Lin, S. J.: Sources and distributions of dust aerosols simulated with the GOCART model, J Geophys Res-Atmos, 106, https://doi.org/20255-20273, 2001.

Ginoux, P., Prospero, J. M., Torres, O., and Chin, M.: Long-term simulation of global dust distribution with the GOCART model: correlation with North Atlantic Oscillation, Environ Modell Softw, 19, 113-128, https://doi.org/10.1016/S1364-8152(03)00114-2, 2004.

Ginoux, P., Prospero, J. M., Gill, T. E., Hsu, N. C., and Zhao, M.: Global-Scale Attribution of Anthropogenic and Natural Dust Sources and Their Emission Rates Based on Modis Deep Blue Aerosol Products, Rev Geophys, 50, Artn Rg3005, https://doi.org/10.1029/2012rg000388, 2012.

Huneeus, N., Schulz, M., Balkanski, Y., Griesfeller, J., Prospero, J., Kinne, S., Bauer, S., Boucher, O., Chin, M., Dentener, F., Diehl, T., Easter, R., Fillmore, D., Ghan, S., Ginoux, P., Grini, A., Horowitz, L., Koch, D., Krol, M. C., Landing, W., Liu, X., Mahowald, N., Miller, R., Morcrette, J. J., Myhre, G., Penner, J., Perlwitz, J., Stier, P., Takemura, T., and Zender, C. S.: Global dust model intercomparison in AeroCom phase I, Atmos Chem Phys, 11, 7781-7816, https://doi.org/10.5194/acp-11-7781-2011, 2011.

Hurrell, J. W., Holland, M. M., Gent, P. R., Ghan, S., Kay, J. E., Kushner, P. J., Lamarque, J. F., Large, W. G., Lawrence, D., Lindsay, K., Lipscomb, W. H., Long, M. C., Mahowald, N., Marsh, D. R., Neale, R. B., Rasch, P., Vavrus, S., Vertenstein, M., Bader, D., Collins, W. D., Hack, J. J., Kiehl, J., and Marshall, S.: The Community Earth System Model: A Framework for Collaborative Research, Bulletin of the American Meteorological Society, 94, 1339-1360, https://doi.org/10.1175/BAMS-D-12-00121.1, 2013.

Jickells, T. D., An, Z. S., Andersen, K. K., Baker, A. R., Bergametti, G., Brooks, N., Cao, J. J., Boyd, P. W., Duce, R. A., Hunter, K. A., Kawahata, H., Kubilay, N., laRoche, J., Liss, P. S., Mahowald, N., Prospero, J. M., Ridgwell, A. J., Tegen, I., and Torres, R.: Global Iron Connections Between Desert Dust, Ocean Biogeochemistry, and Climate, 308, 67-71, https://doi.org/10.1126/science.1105959 %J Science, 2005.

Kohfeld, K. E., and Harrison, S. P.: DIRTMAP: the geological record of dust, Earth-Science Reviews, 54, 81-114, https://doi.org/10.1016/S0012-8252(01)00042-3, 2001.

Lin, Z. H., Levy, J. K., Lei, H., and Bell, M. L.: Advances in Disaster Modeling, Simulation and Visualization for Sandstorm Risk Management in North China, Remote Sens-Basel, 4, 1337-1354, https://doi.org/10.3390/Rs4051337, 2012.

Liu, X., Easter, R. C., Ghan, S. J., Zaveri, R., Rasch, P., Shi, X., Lamarque, J. F., Gettelman, A., Morrison, H., Vitt, F., Conley, A., Park, S., Neale, R., Hannay, C.,

https://doi.org/10.5194/acp-2020-179
Preprint. Discussion started: 3 April 2020

Ekman, A. M. L., Hess, P., Mahowald, N., Collins, W., Iacono, M. J., Bretherton, C. S., Flanner, M. G., and Mitchell, D.: Toward a minimal representation of aerosols in climate models: description and evaluation in the Community Atmosphere Model CAM5, Geosci. Model Dev., 5, 709-739, https://doi.org/10.5194/gmd-5-709-2012, 2012a.

Liu, X., Shi, X., Zhang, K., Jensen, E. J., Gettelman, A., Barahona, D., Nenes, A., and Lawson, P.: Sensitivity studies of dust ice nuclei effect on cirrus clouds with the Community Atmosphere Model CAM5, Atmos. Chem. Phys., 12, 12061-12079, https://doi.org/10.5194/acp-12-12061-2012, 2012b.

Maenhaut, W., Fernández-Jiménez, M. T., Rajta, I., Dubtsov, S., Meixner, F. X., Andreae, M. O., Torr, S., Hargrove, J. W., Chimanga, P., and Mlambo, J.: Long-term aerosol composition measurements and source apportionment at Rukomechi, Zimbabwe, Journal of Aerosol Science, 31, 228-229, https://doi.org/10.1016/S0021-8502(00)90237-4, 2000a.

Maenhaut, W., Fernández-Jiménez, M. T., Vanderzalm, J. L., Hooper, B., Hooper, M. A., and Tapper, N. J.: Aerosol composition at Jabiru, Australia, and impact of biomass burning, Journal of Aerosol Science, 31, 745-746, https://doi.org/10.1016/S0021-8502(00)90755-9, 2000b.

Mahowald, N., Kohfeld, K., Hansson, M., Balkanski, Y., Harrison, S. P., Prentice, I. C., Schulz, M., and Rodhe, H.: Dust sources and deposition during the last glacial maximum and current climate: A comparison of model results with paleodata from ice cores and marine sediments, 104, 15895-15916, https://doi.org/10.1029/1999jd900084, 1999.

Mahowald, N., Ward, D. S., Kloster, S., Flanner, M. G., Heald, C. L., Heavens, N. G., Hess, P. G., Lamarque, J. F., and Chuang, P. Y.: Aerosol Impacts on Climate and Biogeochemistry, Annu Rev Env Resour, 36, 45-74, https://doi.org/10.1146/annurev-environ-042009-094507, 2011.

Mahowald, N. M., Engelstaedter, S., Luo, C., Sealy, A., Artaxo, P., Benitez-Nelson, C., Bonnet, S., Chen, Y., Chuang, P. Y., Cohen, D. D., Dulac, F., Herut, B., Johansen, A. M., Kubilay, N., Losno, R., Maenhaut, W., Paytan, A., Prospero, J. M., Shank, L. M., and Siefert, R. L.: Atmospheric Iron Deposition: Global Distribution, Variability, and Human Perturbations, 1, 245-278, https://doi.org/10.1146/annurev.marine.010908.163727, 2009.

Marticorena, B., and Bergametti, G.: Modeling the Atmospheric Dust Cycle .1. Design of a Soil-Derived Dust Emission Scheme, J Geophys Res-Atmos, 100, 16415-16430, 1995.

Martin, G. M., Bellouin, N., Collins, W. J., Culverwell, I. D., Halloran, P. R., Hardiman,

S. C., Hinton, T. J., Jones, C. D., McDonald, R. E., McLaren, A. J., O'Connor, F. M., Roberts, M. J., Rodriguez, J. M., Woodward, S., Best, M. J., Brooks, M. E., Brown, A. R., Butchart, N., Dearden, C., Derbyshire, S. H., Dharssi, I., Doutriaux-Boucher, M., Edwards, J. M., Falloon, P. D., Gedney, N., Gray, L. J., Hewitt, H. T., Hobson, M., Huddleston, M. R., Hughes, J., Ineson, S., Ingram, W. J., James, P. M., Johns, T. C., Johnson, C. E., Jones, A., Jones, C. P., Joshi, M. M., Keen, A. B., Liddicoat, S., Lock, A. P., Maidens, A. V., Manners, J. C., Milton, S. F., Rae, J. G. L., Ridley, J. K., Sellar, A., Senior, C. A., Totterdell, I. J., Verhoef, A., Vidale, P. L., and Wiltshire, A.: The HadGEM2 family of Met Office Unified Model climate configurations, Geosci. Model Dev., 4, 723-757, https://doi.org/10.5194/gmd-4-723-2011, 2011.

Miller, R. L., Cakmur, R. V., Perlwitz, J., Geogdzhayev, I. V., Ginoux, P., Koch, D., Kohfeld, K. E., Prigent, C., Ruedy, R., Schmidt, G. A., and Tegen, I.: Mineral dust aerosols in the NASA Goddard Institute for Space Sciences ModelE atmospheric general circulation model, Journal of Geophysical Research: Atmospheres, 111, https://doi.org/10.1029/2005JD005796, 2006.

Nyanganyura, D., Maenhaut, W., Mathuthu, M., Makarau, A., and Meixner, F. X.: The chemical composition of tropospheric aerosols and their contributing sources to a continental background site in northern Zimbabwe from 1994 to 2000, Atmos Environ, 41, 2644-2659, https://doi.org/10.1016/j.atmosenv.2006.11.015, 2007.

Prospero J M.: The Atmospheric transport of particles to the Ocean, in Particle Flux in the Ocean, edited by Ittekkot V, Schäfer P, Honjo S, .and Depetris P J, SCOPE Report 57, John Wiley & Sons, Chichester, 19-52, 1996.

Prospero, J. M., Ginoux, P., Torres, O., Nicholson, S. E., and Gill, T. E.: ENVIRONMENTAL CHARACTERIZATION OF GLOBAL SOURCES OF ATMOSPHERIC SOIL DUST IDENTIFIED WITH THE NIMBUS 7 TOTAL OZONE MAPPING SPECTROMETER (TOMS) ABSORBING AEROSOL PRODUCT, 40, 2-1-2-31, https://doi.org/10.1029/2000rg000095, 2002.

Pu, B., and Ginoux, P.: How reliable are CMIP5 models in simulating dust optical depth?, Atmos. Chem. Phys. Discuss., 2018, 1-60, 10.5194/acp-2018-242, 2018.

Rahimi, S., Liu, X., Wu, C., Lau, W. K., Brown, H., Wu, M., and Qian, Y.: Quantifying snow darkening and atmospheric radiative effects of black carbon and dust on the South Asian monsoon and hydrological cycle: experiments using variable-resolution CESM, Atmos. Chem. Phys., 19, 12025-12049, https://doi.org/10.5194/acp-19-12025-2019, 2019.

Randles, C. A., Silva, A. M. d., Buchard, V., Colarco, P. R., Darmenov, A., Govindaraju, R., Smirnov, A., Holben, B., Ferrare, R., Hair, J., Shinozuka, Y., and Flynn, C. J.: The MERRA-2 Aerosol Reanalysis, 1980 Onward. Part I: System Description and

Data Assimilation Evaluation, 30, 6823-6850, https://doi.org/10.1175/jcli-d-16-0609.1, 2017.

Rotstayn, L. D., Jeffrey, S. J., Collier, M. A., Dravitzki, S. M., Hirst, A. C., Syktus, J. I., and Wong, K. K.: Aerosol- and greenhouse gas-induced changes in summer rainfall and circulation in the Australasian region: a study using single-forcing climate simulations, Atmos. Chem. Phys., 12, 6377-6404, https://doi.org/10.5194/acp-12-6377-2012, 2012.

Ryder, C. L., Marenco, F., Brooke, J. K., Estelles, V., Cotton, R., Formenti, P., McQuaid, J. B., Price, H. C., Liu, D., Ausset, P., Rosenberg, P. D., Taylor, J. W., Choularton, T., Bower, K., Coe, H., Gallagher, M., Crosier, J., Lloyd, G., Highwood, E. J., and Murray, B. J.: Coarse-mode mineral dust size distributions, composition and optical properties from AER-D aircraft measurements over the tropical eastern Atlantic, Atmos. Chem. Phys., 18, 17225-17257, https://doi.org/10.5194/acp-18-17225-2018, 2018.

Sakamoto, T. T., Komuro, Y., Nishimura, T., Ishii, M., Tatebe, H., Shiogama, H., Hasegawa, A., Toyoda, T., Mori, M., Suzuki, T., Imada, Y., Nozawa, T., Takata, K., Mochizuki, T., Ogochi, K., Emori, S., Hasumi, H., and Kimoto, M.: MIROC4h - A New High-Resolution Atmosphere-Ocean Coupled General Circulation Model, Journal of the Meteorological Society of Japan. Ser. II, 90, 325-359, https://doi.org/10.2151/jmsj.2012-301, 2012.

Schmidt, G. A., Kelley, M., Nazarenko, L., Ruedy, R., Russell, G. L., Aleinov, I., Bauer, M., Bauer, S. E., Bhat, M. K., Bleck, R., Canuto, V., Chen, Y.-H., Cheng, Y., Clune, T. L., Del Genio, A., de Fainchtein, R., Faluvegi, G., Hansen, J. E., Healy, R. J., Kiang, N. Y., Koch, D., Lacis, A. A., LeGrande, A. N., Lerner, J., Lo, K. K., Matthews, E. E., Menon, S., Miller, R. L., Oinas, V., Oloso, A. O., Perlwitz, J. P., Puma, M. J., Putman, W. M., Rind, D., Romanou, A., Sato, M., Shindell, D. T., Sun, S., Syed, R. A., Tausnev, N., Tsigaridis, K., Unger, N., Voulgarakis, A., Yao, M.-S., and Zhang, J.: Configuration and assessment of the GISS ModelE2 contributions to the CMIP5 archive, Journal of Advances in Modeling Earth Systems, 6, 141-184, https://doi.org/10.1002/2013MS000265, 2014.

Shao, Y.: Physics and modelling of wind erosion, Springer, Berlin, Germany, 2008.

Shao, Y., Leys, J. F., McTainsh, G. H., and Tews, K.: Numerical simulation of the October 2002 dust event in Australia, 112, 10.1029/2006jd007767, 2007.

Shao, Y., Raupach, M. R., & Leys, J. F. (1996). A model for predicting aeolian sand drift and dust entrainment on scales from paddock to region, Australian Journal of Soil Research, 34(3), 309-342, https://doi.org/10.10.71/SR9960309, 1996.

Shao, Y. P., Wyrwoll, K. H., Chappell, A., Huang, J. P., Lin, Z. H., McTainsh, G. H.,

Mikami, M., Tanaka, T. Y., Wang, X. L., and Yoon, S.: Dust cycle: An emerging core theme in Earth system science, Aeolian Res, 2, 181-204, https://doi.org/10.1016/j.aeolia.2011.02.001, 2011.
Takemura, T., Okamoto, H., Maruyama, Y., Numaguti, A., Higurashi, A., and Nakajima, T.: Global three-dimensional simulation of aerosol optical thickness distribution of various origins, Journal of Geophysical Research: Atmospheres, 105, 17853-17873, https://doi.org/10.1029/2000JD900265, 2000.
Takemura, T., Egashira, M., Matsuzawa, K., Ichijo, H., O'Ishi, R., and Abe-Ouchi, A.: A simulation of the global distribution and radiative forcing of soil dust aerosols at the Last Glacial Maximum, Atmos. Chem. Phys., 9, 3061-3073, https://doi.org/10.5194/acp-9-3061-2009, 2009.
Tanaka, T. Y., and Chiba, M.: Global Simulation of Dust Aerosol with a Chemical Transport Model, MASINGAR, Journal of the Meteorological Society of Japan. Ser. II, 83A, 255-278, 10.2151/jmsj.83A.255, 2005.
Tanaka, T. Y., and Chiba, M.: A numerical study of the contributions of dust source regions to the global dust budget, Global Planet Change, 52, 88-104, https://doi.org/10.1016/j.gloplacha.2006.02.002, 2006.
Vanderzalm, J. L., Hooper, M. A., Ryan, B., Maenhaut, W., Martin, P., Rayment, P. R., and Hooper, B. M.: Impact of seasonal biomass burning on air quality in the ”Top End” of regional Northern Australia, Clean Air and Environmental Quality, 37(3), 28–34, 2003.
von Salzen, K., Scinocca, J. F., McFarlane, N. A., Li, J., Cole, J. N. S., Plummer, D., Verseghy, D., Reader, M. C., Ma, X., Lazare, M., and Solheim, L.: The Canadian Fourth Generation Atmospheric Global Climate Model (CanAM4). Part I: Representation of Physical Processes, Atmosphere-Ocean, 51, 104-125, https://doi.org/10.1080/07055900.2012.755610, 2013.
Watanabe, M., Suzuki, T., O’ishi, R., Komuro, Y., Watanabe, S., Emori, S., Takemura, T., Chikira, M., Ogura, T., Sekiguchi, M., Takata, K., Yamazaki, D., Yokohata, T., Nozawa, T., Hasumi, H., Tatebe, H., and Kimoto, M.: Improved Climate Simulation by MIROC5: Mean States, Variability, and Climate Sensitivity, J Climate, 23, 6312-6335, https://doi.org/10.1175/2010jcli3679.1, 2010.
Watanabe, S., Hajima, T., Sudo, K., Nagashima, T., Takemura, T., Okajima, H., Nozawa, T., Kawase, H., Abe, M., Yokohata, T., Ise, T., Sato, H., Kato, E., Takata, K., Emori, S., and Kawamiya, M.: MIROC-ESM 2010: model description and basic results of CMIP5-20c3m experiments, Geosci. Model Dev., 4, 845-872, https://doi.org/10.5194/gmd-4-845-2011, 2011.
Woodward, S.: Modeling the atmospheric life cycle and radiative impact of mineral dust

https://doi.org/10.5194/acp-2020-179
Preprint. Discussion started: 3 April 2020

Atmospheric Chemistry and Physics Discussions

in the Hadley Centre climate model, Journal of Geophysical Research: Atmospheres, 106, 18155-18166, https://doi.org/10.1029/2000JD900795, 2001.

Woodward, S.: Mineral dust in HadGEM2, Hadley Centre tech. Note 87. Met Office, Exeter, Devon, UK, 2011.

Wu, C., and Lin, Z.: Uncertainty in Dust Budget over East Asia Simulated by WRF/Chem with Six Different Dust Emission Schemes, Atmospheric and Oceanic Science Letters, 6, 428-433, https://doi.org/10.3878/j.issn.1674-2834.13.0045, 2013.

Wu, C., Lin, Z., He, J., Zhang, M., Liu, X., Zhang, R., and Brown, H.: A process-oriented evaluation of dust emission parameterizations in CESM: Simulation of a typical severe dust storm in East Asia, Journal of Advances in Modeling Earth Systems, 8, 1432-1452, https://doi.org/10.1002/2016MS000723, 2016.

Wu, C., Lin, Z., Liu, X., Li, Y., Lu, Z., and Wu, M.: Can Climate Models Reproduce the Decadal Change of Dust Aerosol in East Asia?, 45, 9953-9962, https://doi.org/10.1029/2018gl079376, 2018a.

Wu, C., Liu, X., Lin, Z., Rahimi-Esfarjani, S. R., and Lu, Z.: Impacts of absorbing aerosol deposition on snowpack and hydrologic cycle in the Rocky Mountain region based on variable-resolution CESM (VR-CESM) simulations, Atmos. Chem. Phys., 18, 511-533, https://doi.org/10.5194/acp-18-511-2018, 2018b.

Wu, M., Liu, X., Yang, K., Luo, T., Wang, Z., Wu, C., Zhang, K., Yu, H., and Darmenov, A.: Modeling Dust in East Asia by CESM and Sources of Biases, 124, 8043-8064, https://doi.org/10.1029/2019jd030799, 2019.

Yue, X., Wang, H. J., Wang, Z. F., and Fan, K.: Simulation of dust aerosol radiative feedback using the Global Transport Model of Dust: 1. Dust cycle and validation, J Geophys Res-Atmos, 114, Artn D10202, https://doi.org/10.1029/2008jd010995, 2009.

Yue, X., Wang, H., Liao, H., and Fan, K.: Simulation of dust aerosol radiative feedback using the GMOD: 2. Dust-climate interactions, 115, https://doi.org/10.1029/2009jd012063, 2010.

Yukimoto, S., Adachi, Y., Hosaka, M., Sakami, T., Yoshimura, H., Hirabara, M., Tanaka, T. Y., Shindo, E., Tsujino, H., Deushi, M., Mizuta, R., Yabu, S., Obata, A., Nakano, H., Koshiro, T., Ose, T., and Kitoh, A.: A New Global Climate Model of the Meteorological Research Institute: MRI-CGCM3—Model Description and Basic Performance, Journal of the Meteorological Society of Japan. Ser. II, 90A, 23-64, https://doi.org/10.2151/jmsj.2012-A02, 2012.

Yukimoto, S., Yoshimura, H., Hosaka, M., Sakami, T., Tsujino, H., Hirabara, M., et al.: Meteorological Research Institute-Earth System Model v1 (MRI-ESM 1)—Model description, Technical Report of MRI, Ibaraki, Japan, 2011.

https://doi.org/10.5194/acp-2020-179
Preprint. Discussion started: 3 April 2020

Atmospheric Chemistry and Physics Discussions

Zender, C. S., Bian, H. S., and Newman, D.: Mineral Dust Entrainment and Deposition (DEAD) model: Description and 1990s dust climatology, J Geophys Res-Atmos, 108, 4416, https://doi.org/10.1029/2002jd002775, 2003.

https://doi.org/10.5194/acp-2020-179
Preprint. Discussion started: 3 April 2020

Atmospheric Chemistry and Physics
Discussions
Open Access
EGU

Table 1. CMIP5 model used in this study. For comparison with CMIP5 models, MERRA-2 reanalysis is also included.

No.	Models[a]	Resolution	Ensemble number	Dust size (in diameter)	Vegetation cover	Dust emission scheme	Model reference
1	ACCESS1-0	1.3° ×1.9°	3	6 bins: 0.0632-0.2-0.632-2-6.32-20-63.2 μm	Prescribed	Woodward (2001, 2011)	Bi et al. (2013) Dix et al. (2013)
2	CanESM2	2.8° ×2.8°	5	2 modes: MMD= 0.78 μm (σ=2) and 3.8 μm (σ=2.15)[b]	Prescribed	Marticorena and Bergametti (1995)	Arora et al. (2011) von Salzen et al. (2013)
3	CESM1-CAM5	0.9° ×1.25°	2	2 modes: 0.1-1-10 μm[c]	Prescribed	Zender et al. (2003)	Hurrell et al. (2013)
4	CSIRO-Mk3-6-0	1.9° ×1.9°	10	4 bins: 0.2-2-4-6-12 μm	Prescribed	Ginoux et al. (2001, 2004)	Rotstayn et al. (2012)
5	GFDL-CM3	2° ×2.5°	5	5 bins: 0.2-2-3.6-6-12-20 μm	Prognostic	Ginoux et al. (2001)	Delworth et al. (2006) Donner et al. (2011)
6	GISS-E2-H	2° ×2.5°	12	4 bins: <2, 2-4-8-16 μm	Prescribed	Cakmur et al. (2006) Miller et al. (2006)	Schmidt et al. (2014)
7	GISS-E2-R	2° ×2.5°	12	4 bins: <2, 2-4-8-16 μm	Prescribed	Cakmur et al. (2006) Miller et al. (2006)	Schmidt et al. (2014)
8	HadGEM2-CC	1.3° ×1.9°	3	6 bins: 0.0632-0.2-0.632-2-6.32-20-63.2 μm	Prognostic	Woodward (2001, 2011)	Collins et al. (2011) Martin et al. (2011)
9	HadGEM2-ES	1.3° ×1.9°	4	As HadGEM2-CC	Prognostic	Woodward (2001, 2011)	Collins et al. (2011) Martin et al. (2011)
10	MIROC4h	0.56° ×0.56°	1	10 bins: 0.2-0.32-0.5-0.8-1.26-2-3.16-5.02-7.96-12.62-20 μm	Prescribed	Takemura et al. (2000)	Sakamoto et al. (2012)
11	MIROC5	1.4° ×1.4°	5	6 bins: 0.2-0.43-0.93-2-4.3-9.3-20 μm	Prescribed	Takemura et al. (2000, 2009)	Watanabe et al. (2010)
12	MIROC-ESM	2.8° ×2.8°	1	As MIROC4h	Prognostic	Takemura et al. (2000, 2009)	Watanabe et al. (2011)
13	MIROC-ESM-CHEM	2.8° ×2.8°	3	As MIROC4h	Prognostic	Takemura et al. (2000, 2009)	Watanabe et al. (2011)
14	MRI-CGCM3	1.1° ×1.1°	5	6 bins: 0.2-0.43-0.93-2-4.3-9.3-20 μm	Prescribed	Shao et al. (1996) Tanaka and Chiba (2005, 2006)	Yukimoto et al. (2011, 2012)

https://doi.org/10.5194/acp-2020-179
Preprint. Discussion started: 3 April 2020

Atmospheric Chemistry and Physics Discussions

15	MRI-ESM1	1.1º ×1.1º	1	6 bins: 0.2-0.43-0.93-2-4.3-9.3-20 μm	Prescribed	Shao et al. (1996) Tanaka and Chiba (2005, 2006)	Yukimoto et al. (2011, 2012) Adachi et al. (2013)
16	MERRA-2	0.5º ×0.625º	1	5 bins: 0.2-2-3.6-6-12-20 μm	Prescribed	Ginoux et al. (2001)	Randles et al. (2017) Buchard et al. (2017)

[a]: Expansions of acronyms: ACCESS1-0, Australian Community Climate and Earth-System Simulator version 1.0; CanESM2, Second Generation Canadian Earth System Model; CESM1-CAM5, Community Earth System Model version 1-Community Atmosphere Model version 5; CSIRO-Mk3-6-0, Commonwealth Scientific and Industrial Research Organization Mark 3.6.0; GFDL-CM3, Geophysical Fluid Dynamics Laboratory Climate Model version 3; GISS-E2-H, Goddard Institute for Space Studies Model E2 coupled with HYCOM (Hybrid Coordinate Ocean Model); GISS-E2-R, Goddard Institute for Space Studies Model E2 coupled with the Russell ocean model; HadGEM2-CC, Hadley Centre Global Environment Model version 2 with Carbon Cycle configuration; HadGEM2-ES, Hadley Centre Global Environment Model version 2 with Earth System configuration; MIROC4h, Model for Interdisciplinary Research on Climate version 4 (high resolution); MIROC5, Model for Interdisciplinary Research on Climate version 5; MIROC-ESM, Model for Interdisciplinary Research on Climate-Earth System Model; MIROC-ESM-CHEM, Model for Interdisciplinary Research on Climate-Earth System Model with Chemistry Coupled; MRI-CGCM3, Meteorological Research Institute Coupled Atmosphere–Ocean General Circulation Model version 3; MRI-ESM1, Meteorological Research Institute Earth System Model version 1.

[b]: MMD is the abbreviation of mass median diameter and σ is geometric standard deviation.

[c]: Dust emission is calculated in the size range of 0.1-1 and 1-10 μm for accumulation and coarse modes, respectively.

Table 2. The location of observational stations for (a) surface dust concentration and (b) fraction of wet deposition used in this study.

(a)

No.	Name	Latitude	Longitude	No.	Name	Latitude	Longitude
1	Miami	25.75ºN	80.25ºW	12	Fanning Island	3.92ºN	159.33ºW
2	Bermuda	32.27ºN	64.87ºW	13	Hawaii	21.33ºN	157.7ºW
3	Barbados	13.17ºN	59.43ºW	14	Jabirun	12.7ºS	132.9ºE
4	Izana Tenerife	28.3ºN	16.5ºW	15	Cape Grim	40.68ºS	144.68ºE
5	Mace Head	53.32ºN	9.85ºW	16	New Caledonia	22.15ºS	167ºE
6	Rukomechi	16ºS	29.5ºE	17	Norfolk Island	29.08ºS	167.98ºE
7	Cheju	33.52ºN	126.48ºE	18	Funafuti	8.5ºS	179.2ºW
8	Hedo	26.92ºN	128.25ºE	19	American Samoa	14.25ºS	170.58ºW
9	Enewetak Atoll	11.33ºN	162.33ºE	20	Cook Islands	21.25ºS	159.75ºW
10	Nauru	0.53ºN	166.95ºE	21	Palmer	64.77ºS	64.05ºW
11	Midway Island	28.22ºN	177.35ºW	22	Mawson	67.6ºS	62.5ºE

(b)

No.	Name	Latitude	Longitude	No.	Name	Latitude	Longitude
1	Bermuda	32.27ºN	64.87ºW	6	New Zealand	34.55ºS	172.75ºE
2	Amsterdam Island	37.83ºS	77.5ºE	7	Midway	28.22ºN	177.35ºW
3	Cape Ferrat	43.68ºN	7.33ºE	8	Fanning	3.92ºN	159.33ºW
4	Enewetak Atoll	11.33ºN	162.33ºE	9	Greenland	65ºN	44ºW
5	Samoa	14.25ºS	170.57ºW	10	Coastal Antartica	75.6ºS	26.8ºW

https://doi.org/10.5194/acp-2020-179
Preprint. Discussion started: 3 April 2020

Atmospheric Chemistry and Physics Discussions

Table 3. Global dust budgets in CMIP5 models.

Model	Emission[a] (Tg/yr)	Wet deposition[b] (Tg/yr)	Burden (Tg)	Life time (day)	Diameter (μm)
ACCESS1-0	2218 (13%)	261 (12%)	8.1	1.3	0.06 - 73
CanESM2	2964 (18%)	882 (30%)	35.8	4.4	Median (0.39, 2)
CESM1-CAM5	3454 (2.0%)	1243 (36%)	24.9	2.6	0.1 - 10
CSIRO-Mk3-6-0	3698 (8.9%)	1024 (28%)	36.1	3.6	0.2 - 12
GFDL-CM3	1246 (10%)	210 (17%)	13.5	4.0	0.1 - 10
GISS-E2-H	1699 (8.2%)	641 (38%)	17.5	3.8	<2 to 16
GISS-E2-R	1677 (8.2%)	625 (37%)	16.9	3.7	<2 to 16
HadGEM2-CC	8186 (11%)	1521 (19%)	41.9	1.9	0.06 - 63
HadGEM2-ES	7972 (10%)	1429 (18%)	41.4	1.9	0.06 - 63
MIROC4h	735 (2.9%)	179 (24%)	2.5	1.4	0.2 – 20
MIROC5	2716 (6.1%)	668 (25%)	19.0	3.0	0.2 – 20
MIROC-ESM	3339 (5.2%)	540 (16%)	15.5	2.0	0.2 – 20
MIROC-ESM-CHEM	3598 (5.2%)	591 (16%)	16.7	2.0	0.2 – 20
MRI-CGCM3	2107 (5.9%)	819 (39%)	14.3	2.5	0.2 – 20
MRI-ESM1	2052 (6.1%)	801 (39%)	13.9	2.5	0.2 – 20
MERRA-2[c]	1620 (7.4%)	692 (38.6%)	20.3	4.1	0.2 – 20

[a]: The global dust emission area fraction is given in parenthesis next to the global dust emission. The dust emission area is defined as the region with the annual mean dust emission flux larger than 1% of global mean annual dust emission flux.

[b]: The ratio of wet deposition to total deposition is given in parenthesis next to wet deposition.

[b]: The global dust deposition is 1692 Tg, which is larger than dust emission because of no adjustment done with dust emission after aerosol assimilation (Section 2).

https://doi.org/10.5194/acp-2020-179
Preprint. Discussion started: 3 April 2020

Atmospheric Chemistry and Physics
Discussions

Table 4. Dust emission amount (Tg) in nine dust source regions. The contribution of each source region to global total dust emission is given in the parenthesis next to dust emission amount.

No.	Models	Global	North Africa	Middle East	Central Asia	South Asia	East Asia	Australia	North America	South America	South Africa
1	ACCESS1-0	2218	1097 (49.5%)	356 (16.1%)	95 (4.3%)	159 (7.2%)	132 (6.0%)	254 (11.4%)	49 (2.2%)	46 (2.1%)	21 (1.0%)
2	CanESM2	2964	1053 (35.5%)	415 (14.0%)	323 (10.9%)	99 (3.3%)	151 (5.1%)	218 (7.3%)	133 (4.5%)	365 (12.3%)	96 (3.2%)
3	CESM1-CAM5	3454	1609 (46.6%)	698 (20.2%)	495 (14.3%)	122 (3.5%)	329 (9.5%)	38 (1.1%)	35 (1.0%)	26 (0.7%)	101 (2.9%)
4	CSIRO-Mk3-6-0	3698	1863 (50.4%)	555 (15.0%)	122 (3.3%)	160 (4.3%)	589 (15.9%)	143 (3.9%)	23 (0.6%)	138 (3.7%)	106 (2.9%)
5	GFDL-CM3	1246	749 (60.1%)	150 (12.1%)	68 (5.4%)	41 (3.3%)	113 (9.1%)	52 (4.2%)	5 (0.4%)	44 (3.6%)	19 (1.5%)
6	GISS-E2-H	1699	1045 (61.5%)	252 (14.8%)	109 (6.4%)	96 (5.7%)	94 (5.5%)	71 (4.2%)	4 (0.3%)	22 (1.3%)	5 (0.3%)
7	GISS-E2-R	1678	1035 (61.7%)	238 (14.2%)	92 (5.5%)	90 (5.4%)	103 (6.1%)	86 (5.1%)	4 (0.2%)	23 (1.4%)	5 (0.3%)
8	HadGEM2-CC	8186	3124 (38.2%)	593 (7.2%)	403 (4.9%)	826 (10.1%)	359 (4.4%)	2278 (27.8%)	264 (3.2%)	196 (2.4%)	142 (1.7%)
9	HadGEM2-ES	7973	3221 (40.4%)	579 (7.3%)	418 (5.2%)	820 (10.3%)	321 (4.0%)	1988 (24.9%)	340 (4.3%)	144 (1.8%)	139 (1.7%)
10	MIROC4h	735	437 (59.4%)	71 (9.7%)	81 (11.1%)	45 (6.1%)	64 (8.8%)	9 (1.2%)	0.1 (0.02%)	3 (0.5%)	24 (3.2%)
11	MIROC5	2716	1762 (64.9%)	269 (9.9%)	175 (6.5%)	96 (3.5%)	243 (8.9%)	26 (1.0%)	4 (0.2%)	79 (2.9%)	61 (2.2%)
12	MIROC-ESM	3339	2627 (78.7%)	244 (7.3%)	72 (2.2%)	30 (0.9%)	273 (8.2%)	0.6 (0.02%)	0.3 (0.008%)	89 (2.6%)	6 (0.2%)
13	MIROC-ESM-CHEM	3598	2719 (75.6%)	274 (7.6%)	84 (2.3%)	44 (1.2%)	362 (10.1%)	1 (0.03%)	0.4 (0.01%)	100 (2.8%)	13 (0.4%)

https://doi.org/10.5194/acp-2020-179
Preprint. Discussion started: 3 April 2020

14	MRI-CGCM3	2107	1146 (54.4%)	258 (12.2%)	22 (1.1%)	174 (8.3%)	390 (18.5%)	55 (2.6%)	2 (0.09%)	49 (2.3%)	11 (0.5%)
15	MRI-ESM1	2052	1108 (54.0%)	246 (12.0%)	21 (1.0%)	167 (8.1%)	392 (19.1%)	57 (2.8%)	2 (0.09%)	48 (2.3%)	10 (0.5%)
16	MERRA-2	1670	1104 (61.1%)	182 (16.2%)	56 (7.7%)	55 (3.1%)	162 (6.3%)	59 (2.6%)	8 (0.5%)	30 (1.7%)	15 (0.7%)

https://doi.org/10.5194/acp-2020-179
Preprint. Discussion started: 3 April 2020

Atmospheric Chemistry and Physics Discussions

Table 5. Total dust deposition and wet deposition in the global surface, continents, and oceans, respectively from CMIP5 models and MERRA-2 reanalysis. Only the seven CMIP5 models with both dry and wet depositions provided are used here.

Model	Global		Continent		Ocean	
	Total	Wet[a]	Total[b]	Wet[a]	Total[b]	Wet[a]
ACCESS1-0	2216	261 (12%)	2019 (91%)	159 (8%)	197 (9%)	102 (52%)
CanESM2	2965	882 (30%)	2279 (77%)	513 (22%)	686 (23%)	369 (54%)
CESM1-CAM5	3454	1243 (36%)	2850 (83%)	945 (33%)	604 (17%)	298 (49%)
GISS-E2-H	1684	641 (38%)	1359 (81%)	410 (30%)	324 (19%)	231 (71%)
GISS-E2-R	1665	625 (37%)	1331 (80%)	392 (29%)	334 (20%)	232 (70%)
MRI-CGCM3	2109	819 (39%)	1649 (78%)	499 (30%)	460 (22%)	319 (69%)
MRI-ESM1	2054	801 (39%)	1609 (78%)	492 (30%)	445 (22%)	309 (69%)
MERRA-2	1792	692 (38.6%)	1272 (71%)	335 (26%)	520 (29%)	356 (69%)

[a]: The ratio of wet deposition to total deposition is given in parenthesis next to wet deposition.
[b]: The fraction of continental (or oceanic) deposition to global deposition is given in next to continental (or oceanic) deposition.

https://doi.org/10.5194/acp-2020-179
Preprint. Discussion started: 3 April 2020

Atmospheric Chemistry and Physics
Discussions
Open Access

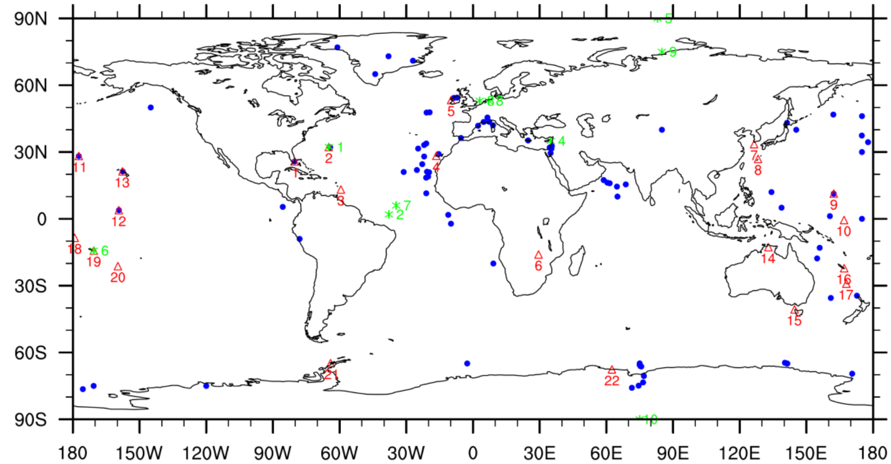

Figure 1. The distribution of observational stations used in this study: blue circles for dust deposition, red triangles for surface dust concentrations, and green asterisks for fraction of wet deposition. The descriptions of all these stations can be found in Section 3.

https://doi.org/10.5194/acp-2020-179
Preprint. Discussion started: 3 April 2020

Atmospheric Chemistry and Physics Discussions
Open Access
EGU

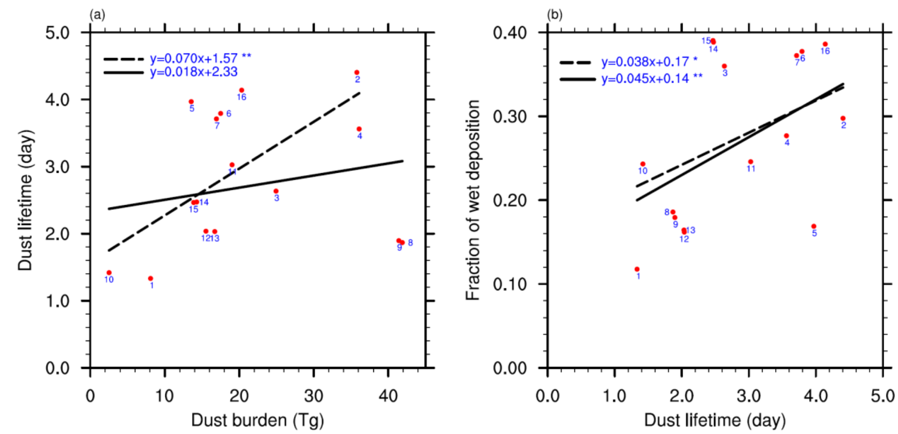

Figure 2. Scatter plot of (a) dust burden versus dust life time and (b) dust life time versus fraction of wet deposition to total deposition in 15 CMIP5 models and in MERRA-2 reanalysis. The models are indexed as Table 1. The regression lines from all the CMIP5 models (solid) and the CMIP5 models excluding HadGEM2-CC/ES models (dash) are also shown with the slopes and intercepts for the regression equation. Significant test for each regression is denoted by one asterisk (*; above significant level of 0.1) and two asterisks (**; above significant level of 0.05) after each regression equation.

https://doi.org/10.5194/acp-2020-179
Preprint. Discussion started: 3 April 2020

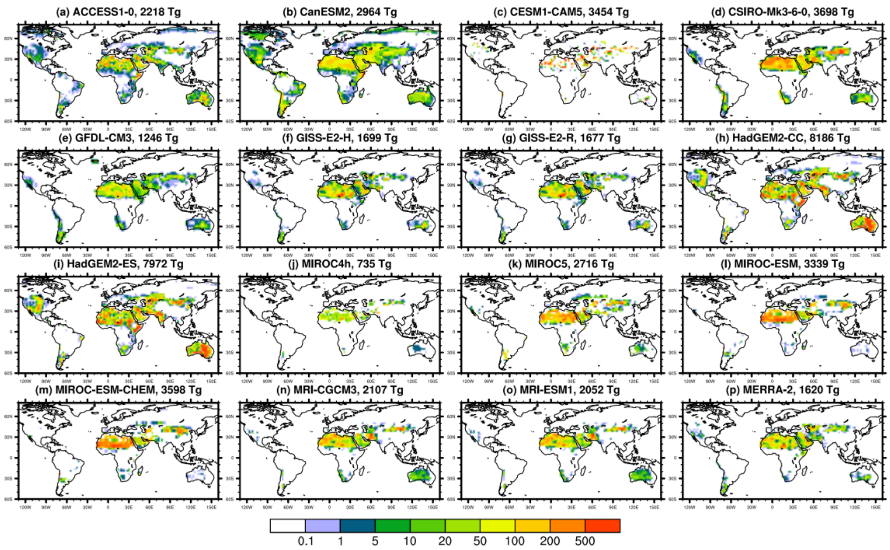

Figure 3. (a-o) Annual mean dust emission flux (g m^{-2} yr^{-1}) during 1960-2005 from 15 CMIP5 models, and (p) annual mean dust emission (g m^{-2} yr^{-1}) during 1980-2018 from MERRA-2 reanalysis. The total annual global dust emission is included in the title of each panel.

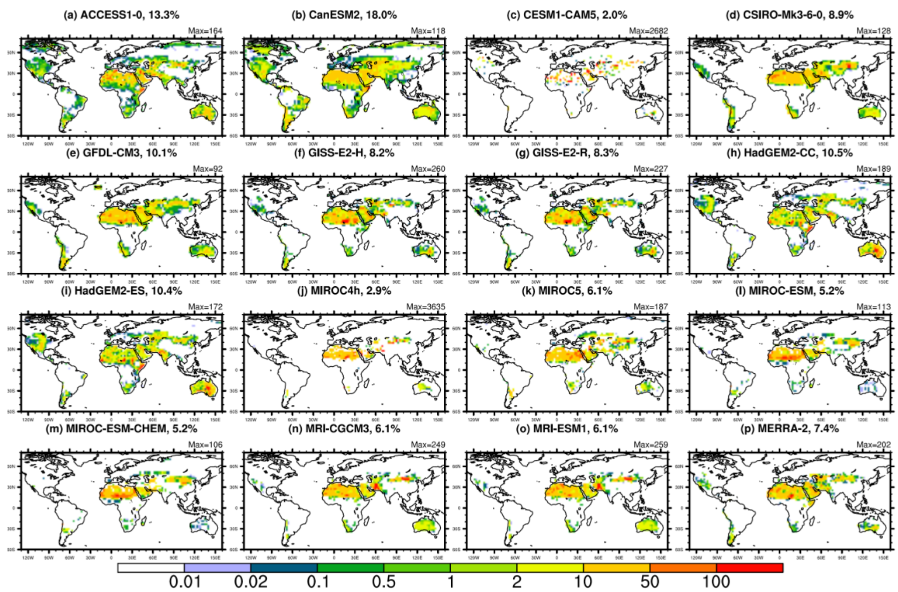

Figure 4. Normalized dust emission flux in 15 CMIP5 models and MERRA-2 reanalysis. Normalized dust emission flux is calculated from dust emission flux divided by global mean for each model. The percentage of dust source area relative to global total surface area is given in the title of each panel. Dust source area is defined as the normalized dust emission flux greater than 0.01. The maximum normalized dust emission flux is also given in the top right corner of each panel.

https://doi.org/10.5194/acp-2020-179
Preprint. Discussion started: 3 April 2020

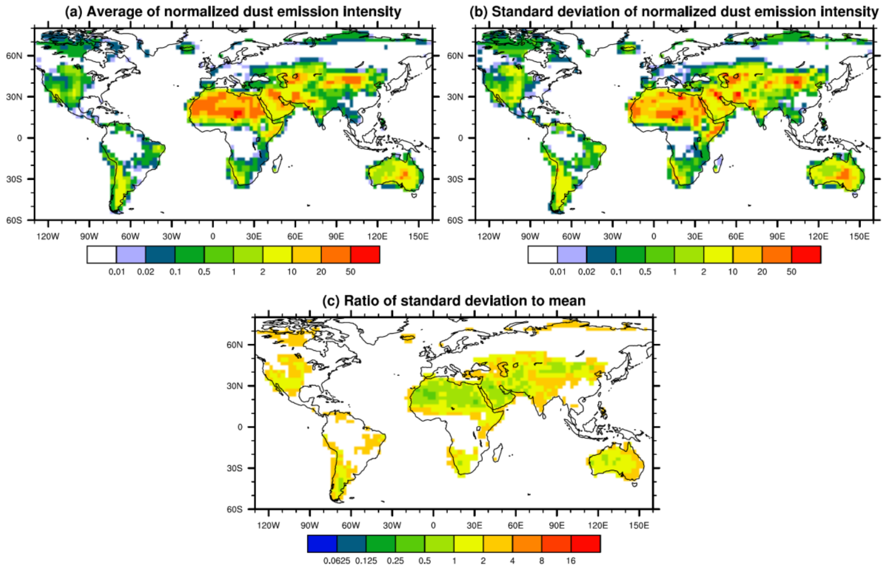

1019

1020 **Figure 5.** Mean, standard deviation, and relative standard deviation (also known as
1021 coefficient of variation) of normalized dust emission flux from 15 CMIP5 models.
1022 Relative standard deviation is derived by calculating the ratio of standard deviation to
1023 mean.

1024

https://doi.org/10.5194/acp-2020-179
Preprint. Discussion started: 3 April 2020

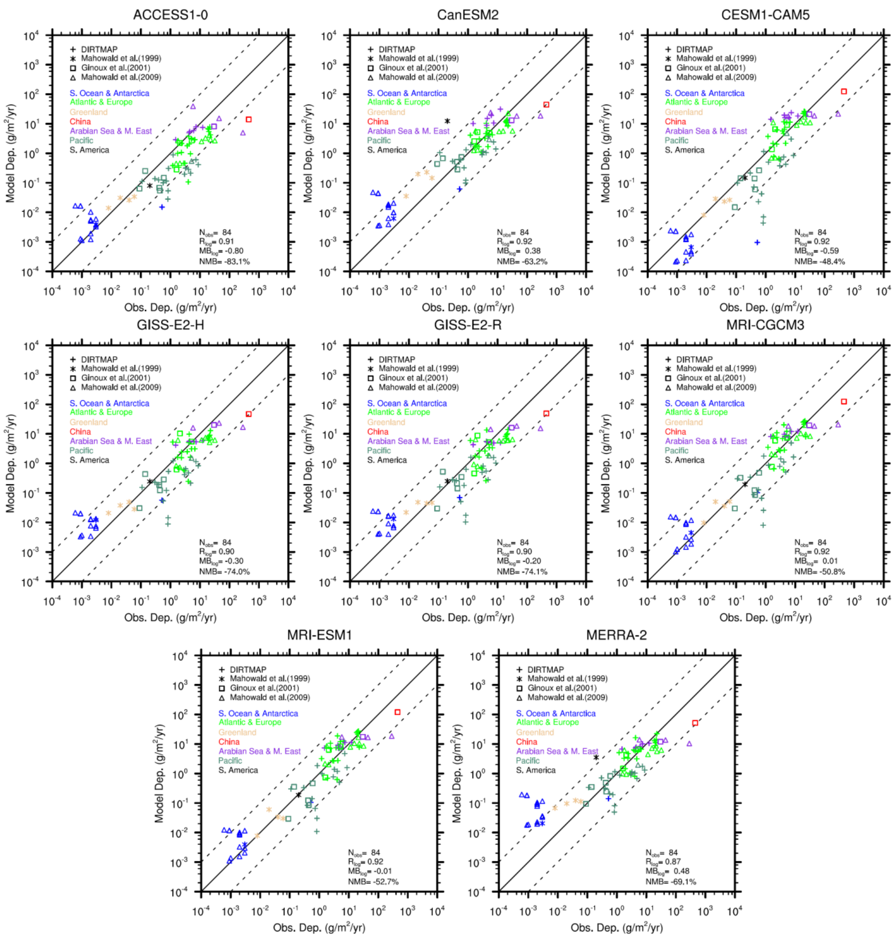

Figure 6. Scatterplot of dust deposition flux at 84 selected stations between models and observations. The stations are marked with different styles according to the sources of data and with different colors for different locations (Section 3). Also given are the correlation coefficients and mean bias between models and observations (after taking the logarithms; R_{log} and MB_{log}, respectively). The normalized mean bias (NMB) that is calculated from the mean bias divided by mean observations is given as well. The 1:1 (solid) and 1:10/10:1 (dash) lines are plotted for reference.

https://doi.org/10.5194/acp-2020-179
Preprint. Discussion started: 3 April 2020

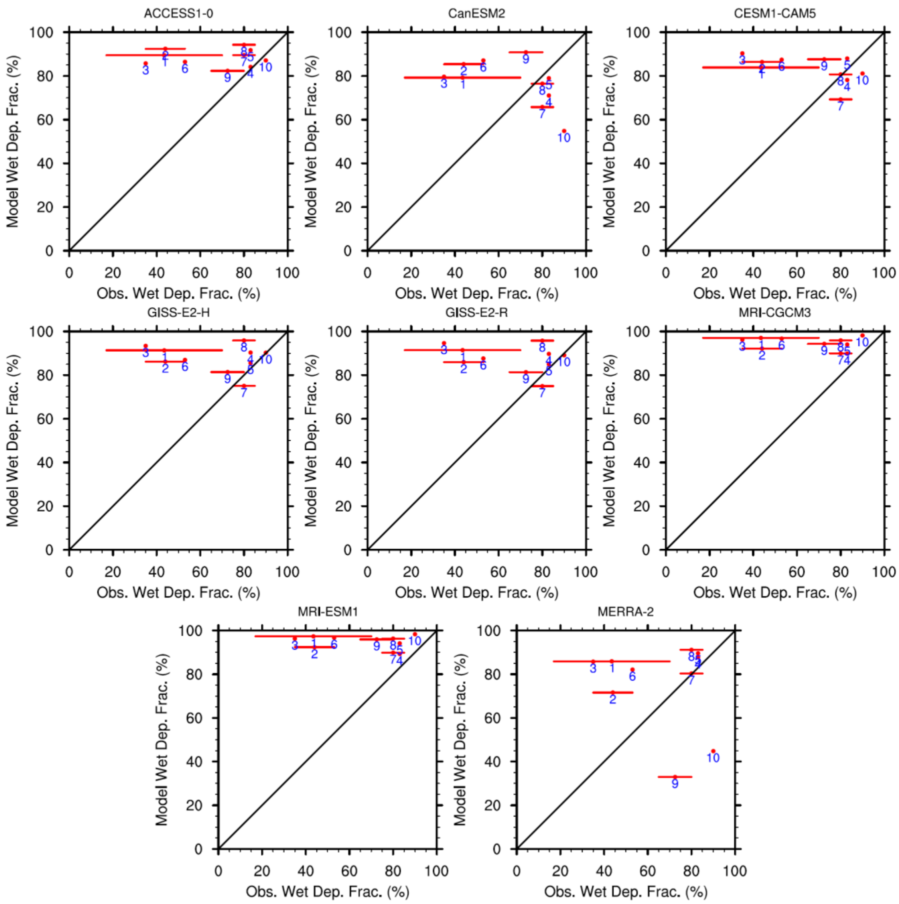

Figure 7. Scatterplot of fraction of wet deposition in total deposition between models and observations. For the observations that provide the minimum and maximum values, the mean of minimum and maximum values is used with the ranges indicated by a horizontal line. Station numbers are indexed following Table 2.

https://doi.org/10.5194/acp-2020-179
Preprint. Discussion started: 3 April 2020

Atmospheric Chemistry and Physics
Discussions

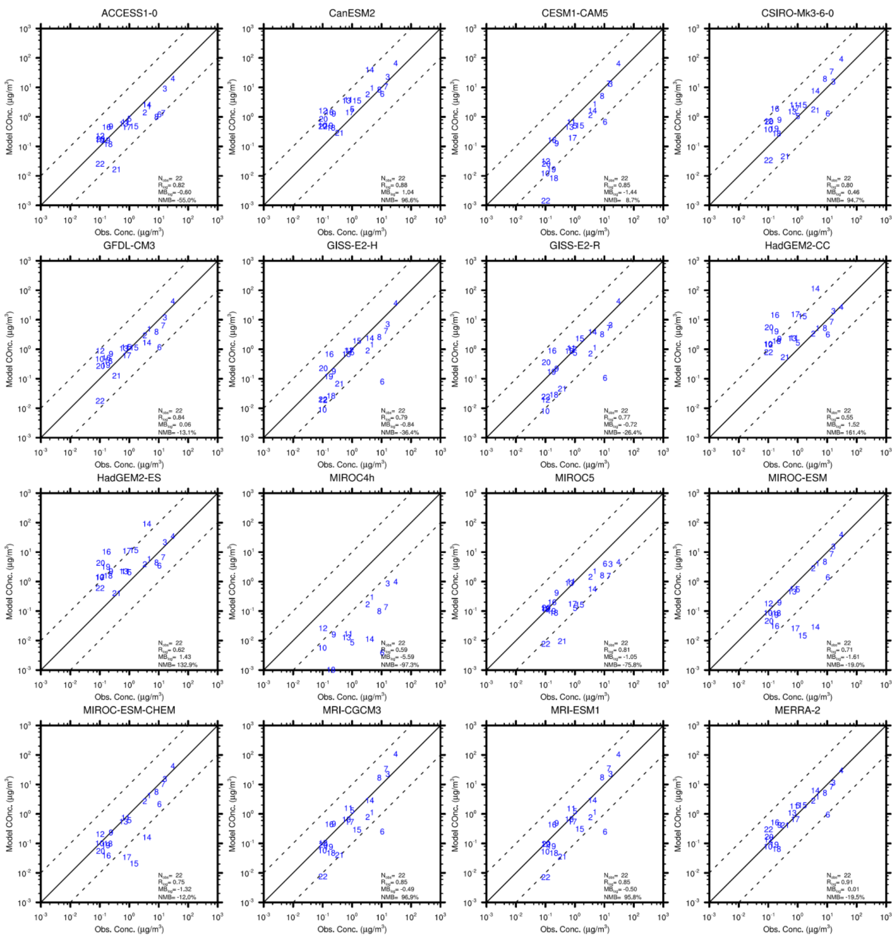

Figure 8. Scatterplot of surface dust concentration at 22 selected stations between models and observations. The stations are indexed as Table 2 and their locations are shown in Figure 1. Also given are the correlation coefficients and mean bias between models and observations (after taking the logarithms; R_{log} and MB_{log}, respectively). The normalized mean bias (NMB) that is calculated from the mean bias divided by mean observations is given as well. The 1:1 (solid) and 1:10/10:1 (dash) lines are plotted for reference. The comparison results for some stations (#15-17 and #19-22 for MIROC4h; #21 and #22 for MIROC-ESM and MIROC-ESM-CHEM) are not shown as they are located too low and outside the frame.